UNIVERSITÉ DU QUÉBEC À MONTRÉAL

MARÉES ROUGES ET DISTRIBUTION DES ASSEMBLAGES PALYNOLOGIQUES LE LONG DE LA CÔTE OUEST MEXICAINE

MÉMOIRE
PRÉSENTÉ
COMME EXIGENCE PARTIELLE
DE LA MAÎTRISE EN SCIENCES DE LA TERRE

PAR
AUDREY LIMOGES

SEPTEMBRE 2009

REMERCIEMENTS

Je souhaite remercier très sincèrement Anne de Vernal pour la direction de ce projet de maîtrise, sa confiance, ses encouragements et le soutien financier nécessaire à la réalisation de ce travail.

Un grand merci également à Ana Carolina Ruíz-Fernandez pour l'organisation de la campagne d'échantillonage *B/O El Puma* TEHUA V, l'excellent accueil à Mazatlán et son support à distance. Son énergie débordante est une source d'inspiration.

Je tiens spécialement à remercier Taoufik Radi pour son aide et sa participation inestimables tout au long de ce projet. Ses nombreux conseils, sa patience et sa disponibilité au cours des deux dernières années ont grandement contribué à mener à bien cette étude.

Merci à Maryse Henry pour son aide lors des analyses palynologiques.

Merci à mes collègues et amis du laboratoire GEOTOP et particulièrement à Linda Genovesi pour sa précieuse complicité au cours des 2 dernières années. Merci à Benoît Thibodeau pour ses conseils et les nombreux pots massons partagés. Merci à Christelle Not pour son amitié et toute son implication au sein de la vie étudiante. Finalement, un énorme merci à mes parents, mes sœurs et mes beaux-frères pour leur soutien continuel.

AVANT-PROPOS

Ce document présente l'étude *Marées rouges et distribution des assemblages palynologiques le long de la côte Ouest mexicaine* qui a été réalisée dans le cadre d'un projet de collaboration entre le Québec et le Mexique. Cette étude visait l'identification des paramètres environnementaux favorables aux marées rouges et les objectifs spécifiques du projet étaient :

- Développer une base de données de référence de la distribution géographique des kystes de dinoflagellés (dinokystes).

- Caractériser la relation existant entre les assemblages de dinokystes et les paramètres environnementaux du milieu.

Cette étude est présentée sous forme d'article à l'intérieur du chapitre I. Cet article a été soumis à la revue *Marine Micropaleontology*. L'ensemble des échantillonnages, traitements de laboratoire et analyses des sédiments provenant de la marge Ouest mexicaine, ainsi que la rédaction de ce document ont été réalisés par Audrey Limoges. La contribution de chacune des personnes figurant comme co-auteur est la suivante : les données palynologiques obtenues par Kielt (2006) ont été combinées à celles provenant de ce projet afin de développer une base de données de référence plus étendue pour les basses latitudes. Les observations taxonomiques effectuées par Radi Taoufik ont permis de perfectionner la section consacrée à la systématique des dinokystes rencontrés le long de la côte Ouest mexicaine. L'ensemble des opérations d'échantillonnage des sédiments analysés au cours de cette étude a été coordonné par Ana Carolina Ruíz-Fernandez au cours de la mission *B/O El Puma* TEHUA V. Finalement, ce projet a été dirigé par Anne de Vernal.

TABLE DES MATIÈRES

LISTE DES FIGURES

LISTE DES TABLEAUX

LISTE DES APPENDICES

RÉSUMÉ

L'analyse palynologique de 47 échantillons de sédiment de surface provenant de la marge mexicaine (15°95 N à 23°11 N) a été réalisée afin de caractériser la relation existant entre les kystes de dinoflagellés (dinokystes) et les paramètres environnementaux du milieu (température, salinité, productivité primaire, distance par rapport à la côte). Les observations permettent de diviser la zone d'étude en 4 régions caractérisées par des contextes hydrographiques distincts: la baie de La Paz, la marge Ouest mexicaine, le Nord du Golfe de Tehuantepec et le Sud du Golfe de Tehuantepec. Les taxons hétérotrophes dominent l'ensemble de ces assemblages à l'exception de ceux provenant du Sud du Golfe de Tehuantepec. Les concentrations totales de dinokystes suivent un gradient latitudinal décroissant avec des valeurs maximales dans la partie Nord de la zone d'étude.

Les traitements statistiques ont permis de démontrer que la distance par rapport à la côte, ainsi que les valeurs de productivité primaire sont les principaux paramètres déterminant la distribution des kystes de dinoflagellés. Les zones d'upwelling des baies de La Paz et de Tehuantepec présentent plusieurs similarités et leurs assemblages sont dominés par des taxons hétérotrophes tels *Brigantedinium* spp., *Echinidinium* spp, *Polykrikos kofoidii* et *Selenopemphix quanta.* Certaines espèces de dinokystes qui peuvent être à l'origine de marées rouges ont été observées à plusieurs sites. *Lingulodinium machaerophorum* est présent sur la marge Ouest mexicaine et dans le Nord du Golfe de Tehuantepec, alors que les concentrations de *Polysphaeridium zoharyi* sont plus fortes dans la zone d'upwelling du Golfe de Tehuantepec. La distribution des espèces liées aux marées rouges semble être influencée par le niveau de productivité primaire, ainsi que par la richesse en nutriments des eaux de surface.

Mots clés : Mexique, Dinokystes, Marées rouges, Paramètres environnementaux, Productivité primaire.

INTRODUCTION GÉNÉRALE

Le milieu marin de la marge Ouest mexicaine est affecté par de fréquents épisodes de marées rouges. Les organismes planctoniques profitent du grand apport en éléments nutritifs résultant des activités humaines et des processus d'upwelling qui sont particulièrement intenses dans les régions du Golfe de la Californie et du Golfe de Tehuantepec (Mee et al., 1984; Alonso-Rodríguez and Ochoa, 2004). Ce domaine côtier présente une grande diversité de dinoflagellés parmi lesquels certaines espèces produisent des toxines très nocives pour les écosystèmes marins. Le transfert de ces toxines vers les niveaux trophiques supérieurs peut entraîner la mortalité massive des poissons. En plus des conséquences sur les écosystèmes marins, ce phénomène constitue une menace pour les industries de la pêche et du tourisme nationales.

Les dinoflagellés forment un groupe d'organismes planctoniques marins majeur composé d'espèces phototrophes, hétérotrophes et mixotrophes (e.g. Taylor and Pollingher, 1987; Gaines and Elbrachter, 1987). La présence des différentes espèces dans les milieux marins est déterminée par leurs modes de nutrition respectifs : la disponibilité en nutriments et la pénétration de la lumière dans la colonne d'eau sont des caractéristiques du milieu vitales à la croissance des espèces phototrophes, alors que les espèces hétérotrophes dépendent principalement de la présence des diatomées et d'autres micro-organismes qui constituent leurs proies (Jacobson and Anderson, 1986). Au cours de leur période de reproduction, 10 à 20% des dinoflagellés produisent un kyste qui consiste en une enveloppe qui protège leur cellule pour une période de durée variable (Dale, 1976; Taylor and Pollingher, 1987; Head, 1996). Contrairement aux microfossiles carbonatés ou siliceux qui sont très sensibles aux processus de dissolution, les kystes de dinoflagellés (dinokystes) sont composés de matière organique très résistante permettant leur bonne préservation dans les sédiments. Ainsi, suite à des traitements physiques et chimiques effectués sur les sédiments, les dinokystes peuvent être facilement isolés.

En milieu côtier, les assemblages de dinokystes dans les sédiments sont fortement liés aux conditions biotiques et abiotiques de la colonne d'eau. Leur distribution dépend des conditions des eaux de surface telles que la salinité, la température, la durée du couvert de glace et la productivité primaire (de Vernal et al. 1997, 2001, 2005; Rochon et al., 1999; Radi and de Vernal, 2008). Les assemblages de dinokystes ont également été utilisés comme traceurs de la pollution anthropique (urbanisation, industrialisation) et du phénomène d'eutrophisation (Dale and Fjellså, 1994; Dale, 1996).

Étant donné que les dinokystes se sont avérés être des traceurs efficaces pour la réalisation de reconstructions paléocéanographiques et paléoenvironnementales, plusieurs études ont été réalisées pour documenter leur distribution ((Dale and Fjellsä, 1994; Marret, 1994; Devillers and de Vernal, 2000; Radi and de Vernal, 2004; Radi et al., 2007; Pospelova et al., 2008; Zonneveld, 1997; Radi et de Vernal, 2008). Les moyennes et les hautes latitudes ont fait l'objet de plusieurs études (océan Atlantique-Nord, océan Arctique, océan Pacifique-Nord). Cependant, la distribution des dinokystes aux basses latitudes demeure très peu connue. Ainsi, afin d'améliorer la couverture spatiale de la base de donnée de distribution, des analyses palynologiques ont été effectuées sur des sédiments de surface provenant de la marge Ouest mexicaine. Cette région est particulièrement sensible aux marées rouges.

Dans cette étude, nous reportons les analyses palynologiques et géochimiques réalisées sur 47 échantillons de sédiment de surface prélevés à bord du *B/O El Puma* au cours de la campagne océanographique TEHUA V en septembre 2007. Les échantillons proviennent de la zone côtière mexicaine comprise entre le Golfe de la Californie et le Golfe de Tehuantepec (15°95N et 23°11N). Les résultats de cette étude ont été combinés aux données provenant de la Baie de La Paz et du Golfe de Tehuantepec pour le développement d'une base de données de référence des les basses latitudes totalisant 95 sites d'analyse (cf. Kielt, 2006).

CHAPITRE I

RED TIDES AND DINOFLAGELLATE CYST DISTRIBUTION IN SURFACE SEDIMENTS ALONG THE WESTERN MEXICAN COAST (14.76° N TO 24.75°N)

Audrey Limoges[a*], Jean-François Kielt[a], Taoufik Radi[a], Ana Carolina Ruíz-Fernandez[b] and Anne de Vernal[a]

[a] GEOTOP-UQAM-McGill, C.P. 8888, succ. Centre ville, Montréal, Québec, Canada H3C 3P8

[b] Universidad Nacional Autónoma de México, A.P. 811, Centro, 82 000 Mazatlán, Sinaloa, México

*Corresponding author: limoges.audrey@courrier.uqam.ca

ABSTRACT

In this study, we explore the relationship between the modern assemblages of organic-walled dinoflagellate cysts (dinocysts) and sea-surface conditions (temperature, salinity, primary productivity, depth, nearshore-offshore gradient). Statistical treatments were performed on 95 surface sediment samples from sites located along the western Mexican coast (15°95 N to 23°11 N). Redundancy analysis (RDA) illustrates that the principal parameters correlated with the regional dinocyst distribution are the nearshore-offshore gradient and the productivity-level of the upper water column, which is closely related to upwelling. Empirical observations coupled with RDA provide insight about the spatial coverage of some dinocyst taxa produced by dinoflagellate species potentially responsible for harmful algal blooms along the coast. They also allow the recognition of four zones of assemblages, which are linked to upwelling intensity and productivity and characterize La Paz Bay, the western Mexican margin, the northern part of Tehuantepec Gulf and the southern part of Tehuantepec Gulf.

Keywords: Mexico, Dinocysts, Red tides, Environmental parameters, Primary productivity.

1. INTRODUCTION

During the past decades, some areas along the western Mexican coast were affected by periodical and relatively frequent red tide events. Primary productivity is stimulated by upwelling, nutrient enrichment from terrestrial sources and by various biotic and abiotic factors (Mee et al., 1985; Alonso-Rodríguez and Ochoa, 2004). Massive proliferation of toxic dinoflagellates is the major cause of harmful algal blooms (HABs). When high density of toxic species occurs, the toxins are ingested by organisms and transferred to higher trophic levels through the food chain, which may extent until human poisoning. Beside the environmental and human health impacts, HABs represent a big threat for the national tourism and fishing industries.

Dinoflagellates constitute one of the major groups of marine plankton, which include both phototrophic, heterotrophic and mixotrophic species (e.g. Taylor and Pollingher, 1987; Gaines and Elbrachter, 1987). The presence of dinoflagellate species in marine environment depends on their respective feeding behaviours: while phototrophic growth is supported mostly by the nutrient availability and sunlight penetration, heterotrophic species are dependant upon diatoms and other micro-organisms on which they prey (Jacobson and Anderson, 1986). During the reproduction as part of their life-cycle, 10% to 20% of dinoflagellates produce a cyst to protect their cell for a period of time of variable duration (Dale, 1976; Taylor and Pollingher, 1987; Head, 1996). Unlike siliceous or carbonates microfossils, which are sensitive to dissolution processes, the cysts of most dinoflagellates are composed of very resistant organic material and are generally well-preserved in sediment. Therefore, chemical and physical treatments easily allow their extraction from sediments.

In coastal environments, close relationships exist between the modern assemblages of organic-walled dinoflagellate cysts (dinocysts) in sediment and biotic and abiotic conditions in the upper water column. Dinocyst distribution depends upon sea-surface parameters including salinity, temperature, sea-ice cover duration and primary productivity (de Vernal et al. 1997, 2001, 2005; Rochon et al., 1999; Radi and de Vernal, 2008). Dinocyst assemblages

have also been used as tracers of pollution related to human activities (urbanization, industrialization) and development of eutrophication (Dale and Fjellså, 1994; Dale, 1996).

Because dinocyst assemblages from sediments represent a valuable tool for paleoceanographic and paleoenvironmental reconstructions, several studies were undertaken for the establishment of databases (Dale and Fjellsä, 1994; Marret, 1994; Devillers and de Vernal, 2000; Radi and de Vernal, 2004; Radi et al., 2007; Pospelova et al., 2008; Zonneveld, 1997; Radi et de Vernal, 2008). Comprehensive modern reference databases are available for middle to high latitudes (North Atlantic Ocean, Arctic Ocean and North Pacific Ocean) (cf. de Vernal and Marret, 2007). However, the distribution of dinocyst at low latitudes is still poorly documented. Therefore, in order to improve the spatial coverage of the modern dinocyst databases, notably in areas susceptible to record HABs, palynological analyses have been performed in surface sediment from the western Mexican coast.

Here we report on the analyses of 47 surface-sediment samples collected on the B/O *El Puma* during the TEHUA V oceanographic cruise, in September 2007. Sampling sites were located along the western Mexican coast between 15°95 N and 23°11 N and correspond to the area where human activities are developing. The results of the samples analyzed here were combined with data from La Paz Bay and Tehuantepec Bay (cf. Kielt, 2006) to develop a database including a total of 95 sites (Figure 1) (Tables 1-2).

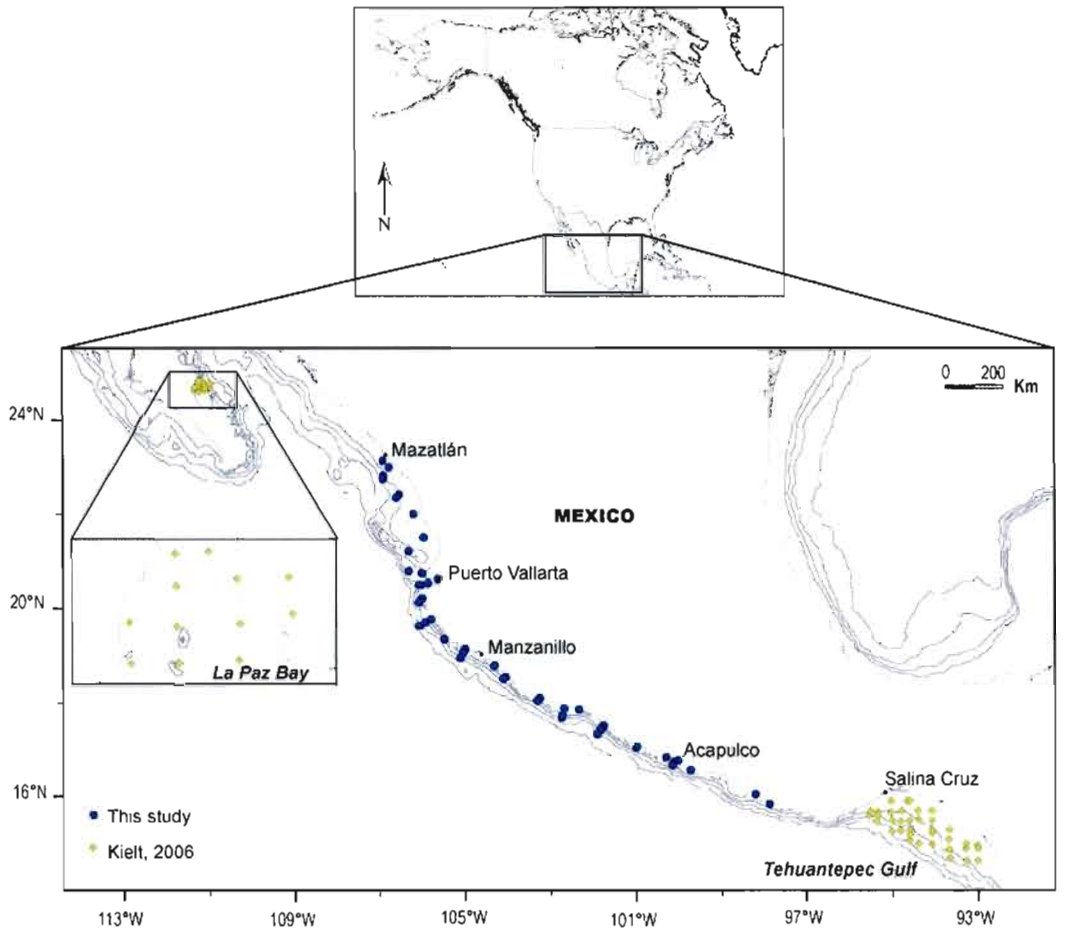

Figure 1. Map of the study area showing the location of the 95 surface-sediment samples used to develop the dinocyst database. The database includes results from this study and from the thesis of Kielt (2006). Isobath contours correspond to 200, 500, 1000 and 2000m.

Table 1. Location of the surface sediment samples investigated in the present study.

Sites	Database number	Laboratory number	Longitude	Latitude	Water depth (m)
TEHUA V 1	13	2407-01	-106.4764	23.1094	61.4
TEHUA V 2	14	2407-02	-106.3356	22.9601	60.7
TEHUA V 3	15	2407-03	-106.4632	22.8055	207.3
TEHUA V 4	16	2407-04	-106.4786	22.7201	366
TEHUA V 6	17	2407-05	-106.1167	22.4000	51.2
TEHUA V 7	18	2407-06	-106.1857	22.3401	74
TEHUA V 8	19	2408-01	-105.7887	21.9958	36.6
TEHUA V 9	20	2408-02	-105.5820	21.5003	60
TEHUA V 10	21	2408-03	-105.8983	21.2167	418.1
TEHUA V 12	22	2408-04	-105.8980	20.8030	422.8
TEHUA V 14	23	2408-05	-105.6111	20.7465	71.6
TEHUA V 15	24	2408-06	-105.6641	20.5241	1400
TEHUA V 16	25	2420-01	-105.4897	20.5495	1127
TEHUA V 16A	26	2420-02	-105.2583	20.6412	278
TEHUA V 17	27	2420-03	-105.6062	20.2345	79.4
TEHUA V 18	28	2420-04	-105.6923	20.1525	204.8
TEHUA V 19	29	2420-05	-105.6700	19.6743	1126
TEHUA V 20	30	2420-06	-105.5407	19.7434	615
TEHUA V 22	31	2421-01	-105.4252	19.8005	77.2
TEHUA V 24	32	2421-03	-105.1253	19.3861	587.6
TEHUA V 25	33	2421-04	-104.6433	19.1485	67.4
TEHUA V 26	34	2421-05	-104.6760	19.1030	228.5
TEHUA V 27	35	2421-06	-104.6945	19.0642	551.8
TEHUA V 28	36	2424-01	-104.7515	18.9636	1188
TEHUA V 29	37	2424-02	-103.9859	18.8270	61.3
TEHUA V 29A	38	2424-03	-104.0086	18.8047	102.6
TEHUA V 30	39	2424-04	-103.7367	18.5726	96.6
TEHUA V 31	40	2424-05	-103.7857	18.5387	191.2
TEHUA V 32	41	2424-06	-102.9745	18.1353	58.5
TEHUA V 33	42	2425-01	-103.0270	18.0886	362.3
TEHUA V 34	43	2425-02	-102.4811	17.7374	713.9
TEHUA V 35	44	2425-03	-102.4687	17.7888	428.9
TEHUA V 36	45	2425-04	-102.4185	17.9154	92.8
TEHUA V 36A	46	2425-05	-102.0956	17.8958	36.5
TEHUA V 37	47	2425-06	-101.5413	17.5747	63.4
TEHUA V 38	48	2426-01	-101.5857	17.5211	173.4
TEHUA V 39	49	2426-02	-101.6063	17.4884	883.1
TEHUA V 40	50	2426-03	-101.6812	17.4089	995.1
TEHUA V 41	51	2426-04	-100.7847	17.1182	153
TEHUA V 43	52	2426-05	-100.7660	17.1382	73
TEHUA V 43A	53	2426-06	-100.1001	16.9214	58.9
Acapulco	54	2427-06	-99.8444	16.8443	24
TEHUA V 44	55	2427-01	-99.9241	16.8138	79.8
TEHUA V 45	56	2427-02	-99.9656	16.7594	241.4
TEHUA V 45A	57	2427-03	-99.5624	16.6484	51.5
TEHUA V 54	58	2427-04	-98.1080	16.1551	72.6
TEHUA V 54A	59	2427-05	-97.7822	15.9525	70.1

Table 2. Location of the surface sediment samples from the study of Kielt (2006).

Sites	Database number	Laboratory number	Longitude	Latitude	Water depth (m)
Paleo IX 22	1	1945-1	-110.7182	24.5440	38.8
Paleo IX 24	2	2098-1	-110.6139	24.5429	334
Paleo IX 26	3	2098-2	-110.4908	24.5508	282
Paleo IX 28	4	1945-2	-110.3758	24.6367	888
Paleo IX 30	5	2098-3	-110.4892	24.6206	34
Paleo IX 32	6	1945-3	-110.6192	24.6123	401
Paleo IX 34	7	2098-4	-110.7184	24.6201	29.5
Paleo IX 35	8	1945-4	-110.6206	24.6891	395
Paleo IX 37	9	2048-5	-110.4943	24.6997	348
Paleo IX 39	10	1945-5	-110.3836	24.7049	850
Paleo IX 43	11	1945-6	-110.5525	24.7547	312
Paleo IX 44	12	2098-6	-110.6226	24.7501	324
TEHUA 1	60	2067-1	-95.5209	15.6995	700
TEHUA 2	61	1946-1	-95.5108	15.7970	225
TEHUA 3	62	2022-4	-95.3202	15.7906	290
TEHUA 4	63	2067-2	-95.3195	15.7011	600
TEHUA 5	64	2030-5	-95.3433	15.5820	1025
TEHUA 6	65	2067-3	-95.0118	15.3642	1050
TEHUA 7	66	2067-5	-95.0052	15.6005	280
TEHUA 8	67	2067-4	-95.0174	15.7683	166
TEHUA 9	68	2068-2	-95.0221	15.9992	67.5
TEHUA 10	69	1946-2	-94.6710	15.9945	68
TEHUA 11	70	2068-3	-94.7999	15.8008	240
TEHUA 12	71	2067-6	-94.8069	15.5920	187
TEHUA 13	72	2068-1	-94.8089	15.3913	230
TEHUA 15	73	1946-3	-94.6182	15.1846	303
TEHUA 16	74	2069-1	-94.6010	15.3965	234
TEHUA 17	75	2068-4	-94.6143	15.6030	230
TEHUA 18	76	2068-5	-94.5999	15.3002	227
TEHUA 19	77	2068-6	-94.5977	15.9992	52
TEHUA 20	78	2022-5	-94.4272	15.8067	95
TEHUA 21	79	2069-2	-94.4080	15.6241	242
TEHUA 23	80	2069-3	-94.4134	15.1121	283
TEHUA 24	81	2030-2	-94.1037	15.1082	245
TEHUA 25	82	2069-4	-94.0997	15.3320	224
TEHUA 26	83	2030-1	-94.0965	15.4092	213
TEHUA 27	84	2069-5	-94.0990	15.6091	110
TEHUA 28	85	2022-6	-94.1007	15.8056	47
TEHUA 29	86	2030-3	-93.7175	15.4026	60
TEHUA 30	87	2069-6	93.7299	15.1972	180
TEHUA 31	88	2070-2	-93.7171	15.0101	187
TEHUA 32	89	2070-1	-93.3369	15.0164	87
TEHUA 33	90	2070-4	-93.3402	15.1202	45
TEHUA 35	91	2030-4	-93.0855	15.0849	35
TEHUA 36	92	2070-3	-93.0840	15.0128	44
TEHUA 37	93	1946-5	-93.0804	14.7638	88
TEHUA 38	94	2070-5	-93.3328	14.7643	258
TEHUA 39	95	2030-6	-93.6940	14.8159	220

2. REGIONAL SETTING

2.1 Oceanographic circulation

Primary productivity in the eastern tropical Pacific is related to the dynamics of water masses, which are determined by atmospheric circulation patterns. The study area can be separated into two important zones: the area influenced by the California Current and the Tehuantepec Gulf (Figure 2).

1- California Bay and the western Mexican coast

The Northern limit of the area under the influence of the California Current is the Colorado River mouth in the California Bay (USA) and the Southern limit is Corrientes Cape in the Mexican region of Sinaloa. From October to May, northwesterly winds induce surface circulation responsible for upwelling on the eastern margin of California Bay and weak upwelling along the western Mexican coast (Barron et al., 2004), which is characterized by warm Tropical water masses (25 to 30°C) flowing southward. Upon reaching 10-20°N, they shift seaward as the Southern branch of the North Pacific subtropical gyre (Kessler, 2006). These waters are characterized by high oxygen concentration and low salinity (33-33.5) (Monreal-Gómez and Salas-de- León, 1998). However, because of the rarity of ocean data, the circulation of water masses is not completely understood during summertime (Kessler, 2006).

2- Gulf of Tehuantepec

The Tehuantepec Gulf is occupied by warm subtropical waters (17 to 30°C), which are characterized by low nutrient concentration and salinity higher than 34.4 (Monreal-Gómez and Salas-de- León, 1998). From early winter to spring (December to May), the hydrology of this area is modulated by northerly strong seasonal winds (Tehuanos) formed in the Mexico Gulf blowing across Central America and passing trough the Isthmus of Tehuantepec (Boumaggard et al., 1998). When the winds reach the Pacific Ocean, they drive intense upwelling in the northern part of Tehuantepec Gulf. Simultaneously, latitudinal shifts of the trade winds system and the Intertropical Convergence Zone (ITCZ) are responsible for large anticyclonic and cyclonic eddies (Arellano-Tores et al., 2003; Monreal-Gómez and Salas-de-

León, 1998). These horizontal and vertical transports trigger the regional biological production by an enhanced nutrient supply. In summer, which is the tropical storms season, the Costa Rica current extends along the coast before turning westward near Corrientes Cape (Kessler, 2006).

2.2 Industrial development along the western Mexican coast

Human activities may severely affect the marine ecosystems with domestic and industrial wastewater discharged in the environment, as well as direct habitat destruction. Besides the urban development related to the fast growing of the populations in the western coastal areas of Mexico, the largest activities susceptible to cause harmful effects to the marine environment are the tourist resorts, harbours and oil-related industries. These activities are particularly thriving in the cities of Mazatlán, Puerto Vallarta, Manzanillo, Acapulco, Puerto Escondido, Puerto Angel and Salina Cruz (Ortiz-Lozano et al., 2005) (see figure 1).

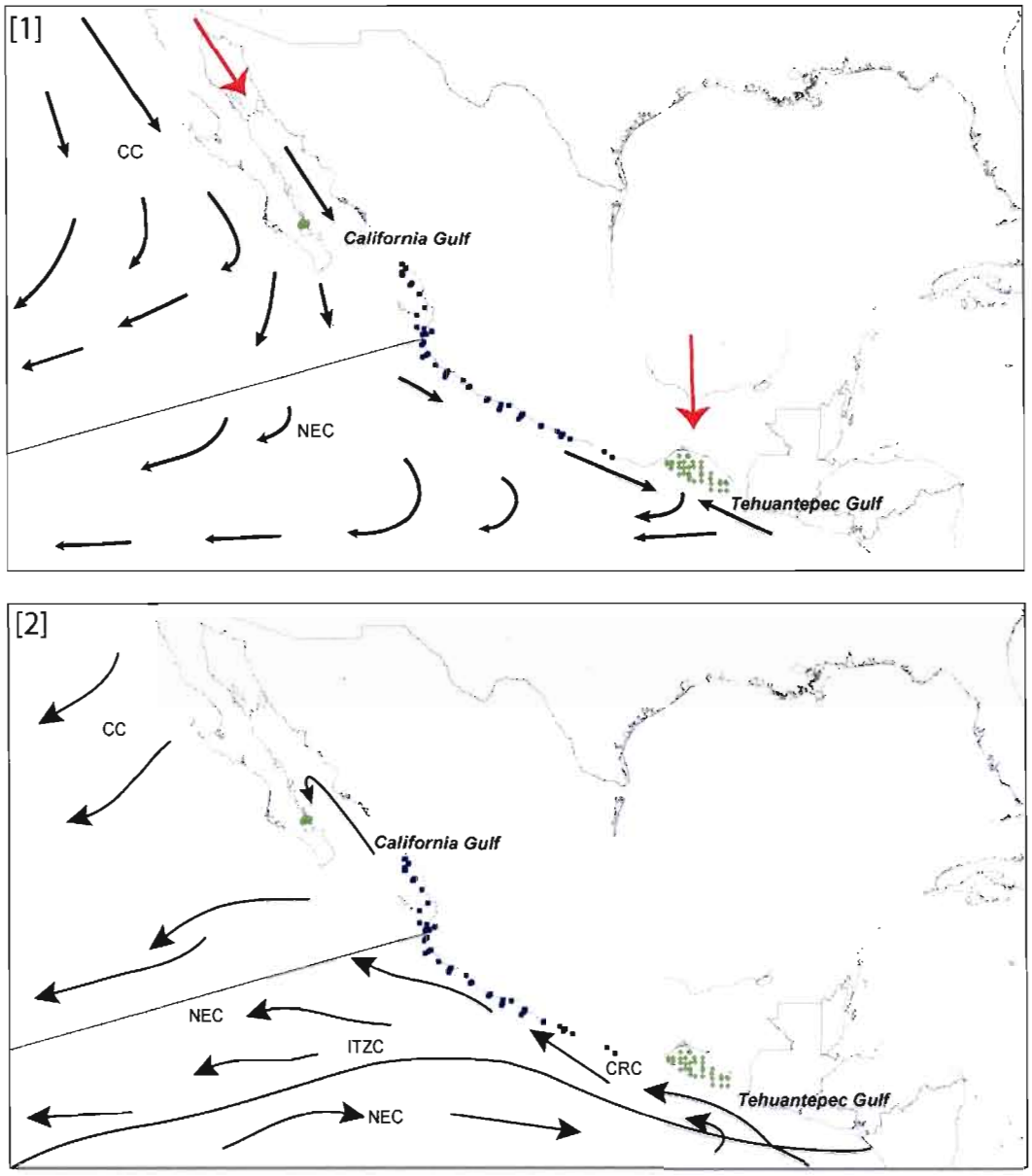

Figure 2. Surface ocean currents of the study area.
(1) Winter-Spring, (2) Summer-Fall. Red arrows correspond to Winter-Spring winds. Current abbreviations are: California Current (CC), Costa Rica Current (CRC), North Equatorial Current (NEC) and Intertropical Convergence Zone (ITZC) (source: Kessler, 2006).

3. MATERIAL AND METHODS

3.1 Sampling

Surface sediments (0-1 cm) were sampled from box cores collected at water depths ranging from 24 to 1400 meters. Wet sediments were stored in a cool room (4°C) until palynological treatments and geochemical analyses. Sediment samples consist in sandy-silty mud and silty-clayed mud.

Sediment mass accumulation rates at the most study sites are unknown. Nevertheless, analyses of ^{210}Pb isotopes have shown that the sedimentation rate is about 0.035 to 0.05 $cm \cdot yr^{-1}$ in La Paz Bay (Douglas et al., 2001) and 0.05 ± 0.01 $cm \cdot yr^{-1}$ in Tehuantepec Bay (Arellano-Torres et al., 2003; Ruiz-Fernàndez et al., 2004). Hence, if we assume similar sedimentation rates at our study sites, we may consider that the upper first centimetre of the box cores represent 20 to 30 years of accumulation on the sea-floor.

3.2 Geochemical analyses

Elemental and isotopic analyses have been performed on surface sediment samples from the Mexican margin exclusively. Prior to geochemical analyses, sediments were dried, crushed with an agate mortar and homogenized. The total carbon (TC) and total nitrogen (TN) composition were determined on 5 to 8 mg of each sediment sample by high temperature combustion using a Carlo Erba™NC2500 elemental analyzer. Analyses of total inorganic carbon (TIC) were made by coulometry on dried and acidified sediments with 1N HCl by which carbonates were removed. Subtracting the total inorganic carbon from the total carbon yields the total organic carbon (TOC) content of a given sample. Replicated measurements of Organic Analytical Standard substances (Acetanilide, Atropine, Cyclohexanone-2, 4-Dinitrophenyl-Hydrazone, Urea and five synthetic mixtures of soil) show a relative deviation of ± 0.1% for the OC and ± 0.3% for TN. The analytical reproducibility corresponds to ± 5%.

Sediment samples for carbon isotopic analysis of organic matter were acidified with 1N HCl, crushed and homogenized. Stable isotope data were obtained using a Carlo Erba™ elemental analyzer coupled to a GV Instrument IsoPrime™ mass spectrometer. Values were reported in

δ-notation (‰) according to the international Vienna-Pee Dee belemnite (VPDB) standard (Coplen, 1995). The $\delta^{13}C$ values were calibrated using two standards: DORM-2 ($\delta^{13}C$ = -28.50‰) and Leucine ($\delta^{13}C$ = -7.35‰) and yielded a relative deviation of ± 0.1‰ (1 σ) vs. V-PDB.

3.3 Palynological analyses

Surface sediment samples were prepared for palynological analyses according to the standardized laboratory procedures suggested by de Vernal et al. (1999). An aliquot of marker grains (*Lycopodium clavatum)* was added to a volume of 5 cm^3 of previously dried sediment. It was sieved with 10 and 106 μm screens to remove debris and particles superior to these size ranges. The fraction of sediment comprised between 10-106 μm was subsequently treated in alternation with hydrochloric acid (HCl 10%) and hydrofluoric acid (HF 48%) in order to dissolve carbonate, silicate and fluorosilicate minerals. The residual fraction of sediment was sieved again to eliminate particles smaller than 10 μm. Then, this residual material was deposed on a glycerin jelly and mounted for observation between a glass slide and a cover-slip.

In most samples, when the dinocyst concentration was sufficient, a minimum of 300 specimens were counted using an optical microscope at 400x to 1000x magnification. The concentrations of pollen grains, foraminifer organic linings and dinocysts were evaluated through the method of Matthews (1969) using the *Lycopodium clavatum* spores and results are expressed as specimens per unit of dry sediment weight (specimens·g^{-1}). According to de Vernal et al. (1987), the reproducibility of the counts is estimated to ± 10% at the 0.95 confidence interval. Dinocyst identification was made in conformity with the nomenclature of Rochon et al. (1999), Radi and de Vernal (2004) and Marret and Zonneveld (2003) (see systematics in Appendix C). Palynological treatments and counts in this study were made following the same procedures than the ones of Kielt (2006) in La Paz Bay and Tehuantepec Gulf. Therefore, both sets of data can be combined to establish a standardized database that includes 95 sites.

3.4 Statistical analyses

Statistical analyses were performed in order to quantitatively determine which environmental variables are controlling the dinocyst abundance and distribution in surface sediments. A detrented correspondence analyse (DCA) was first achieved and revealed that the database follows a linear distribution. Therefore, a redundancy analysis (RDA) was performed using the program CANOCO version 4.0 for Windows. RDA provides information about dinocyst assemblage responses to multiple environmental parameters and allows the determination of the level of influence corresponding to each particular parameter.

The analysis was carried out using the database of the coastal margin of Mexico that includes samples analysed herein in addition to data from Kielt (2006). Three species (*Tuberculodinium vancampoae*, Cyst of *Protoperidinium americanum* and *Dubridinium* spp.) occurring rarely and showing low relative abundances (< 4%) were not used for statistical analyses and some taxa grouping have been made in order to avoid possible bias in the identification between the two studies (Table 3). On the basis of their morphological similarities, cyst of *Protoperidinium nudum* were grouped with *Selenopemphix quanta* and *Polykrikos kofoidii* were grouped with *Polykrikos* cf. *kofoidii*. Similar intraspecific features bring some difficulties in separating *Echinidinium delicatum*, *Echinidinium zonneveldiae* and *Echinidinium transparantum*. Therefore, these species were grouped as *Echinidinum transparantum*. *Echinidinium* cf. *granulatum* and *Echinidinium* sp. x from the analyses of Kielt (2006), as well as *Echinidinium* sp.1 from this study, were grouped with *Echinidinium* spp. Finally, *Spiniferites membranaceus* and *Spiniferites mirabilis* were added to *Spiniferites* spp.

The environmental parameters retained for statistical analyses include temperature, salinity and productivity of surface waters (0 m) as well as the water depth and the distance to the shore of the sampling sites (Table 4).

- Productivity data

Productivity data from the Coastal Zone Color Scanner program (CZCS) (Antoine et al., 1996; Antoine and Morel, 1996) were calculated according to phytoplankton pigment

concentration based on sea-surface color satellite imagery. Uncertainties on the estimates are of the order of 17% (Antoine and Morel, 1996). We also used productivity data from the MODerate resolution Imaging Spectroradiometer (moDIS) program, which were calculated following the Vertical Generalized Primary Production Model (VGPM) developed by Behrenfeld and Falkowski (1997). Interpolations were carried out for sampling sites where productivity values were unavailable from these two datasets.

Comparison between productivity data extracted from the two different sources shows that moDIS-derived estimates of winter and annual productivity are significantly higher than data from the CZCS program. The largest heterogeneity appears in the area between 23°06'561 N and 20°38'471 N, where the difference between the two sensors reaches up to 150 $g \cdot C \cdot m^{-2} \cdot yr^{-1}$ in winter and to 380 $g \cdot C \cdot m^{-2} \cdot yr^{-1}$ for annual averages. These discrepancies may be explained by temporal changes in productivity from one decade to another since data acquisition with the CZCS and moDIS programs were made in 1978-1996 and 2002-2005, respectively; they can also be explained by the algorithms used to estimate productivity through the distinctive methods such as the differences between their respective data acquisition processes and period of observation (see discussion in Radi and de Vernal, 2008).

- Hydrographic parameters

Sea-surface salinity (SSS) and sea-surface temperature (SST) were extracted from the World Ocean Atlas (WOA, 2003) dataset published by the National Climatic Data Center (NCDC). The average values used here were calculated for a radius of 30 nautical miles at a depth of 0 meter. A radius of 60 nautical miles was used for 9 sites where measurements were too sparse.

Table 3. Dinocyst species reported in surface-sediment samples, abbreviations (cf. figure 11) and notes.

Dinocyst species	Abbreviations	Notes
PHOTOTROPHIC SPECIES		
Gonyaulacales		
Bitectatodinium spongium	BSPO	
Lingulodinium machaerophorum	LMAC	
Nematosphaeropsis labyrinthus	NLAB	
Operculodinium centrocarpum	OCEN	
Polyshaeridium zoharyi	PZOH	
Spiniferites delicatus	SDEL	
Spiniferites elongatus	SELO	Grouped with *Spiniferites* spp.
Spiniferites membranaceus	SMEM	Grouped with *Spiniferites* spp.
Spiniferites mirabilis	SMIR	
Spiniferites ramosus	SRAM	
Spiniferites spp.	SSPP	
Tuberculodinium vancampoae	TVAN	Not included in statistical analyses
HETEROTROPHIC SPECIES		
Peridiniales		
Brigantedinium spp.	BSPP	
Cyst of *Pentapharsodinium dalei*	PDAL	
Cyst of *Protoperidinium americanum*	PAME	Not included in statistical analyses
Cyst of *Protoperidinium nudum*	PNUD	Grouped with *S. quanta*
Echinidinium aculeatum	EACU	
Echinidinium delicatum	EDEL	Grouped with *E. transparantum*
Echinidinium granulatum	EGRA	
Echinidinium transparantum	ETRA	
Echinidinium spp.	ESPP	
Lejeunecysta spp.	LSPP	Grouped with Protoperidinioids
Protoperidinioids	PERI	Not included in statistical analyses
Quiquecupsis concreta	QCON	
Selenopemphix nephroides	SNEP	
Selonopemphix quanta	SQUA	
Stelladinium spp.	STSP	
Votadinium spp.	VSPP	
Gymnodiniales et Diplopsalidae		
Cyst of *Gymnodinium catenatum*	GCAT	
Dubridinium spp.	DUBR	Not included in statistical analyses
Polykrikos cf. *kofoidii*	PCKOF	Grouped with *P. kofoidii*
Polykrikos kofoidii	PKOF	
Polykrikos schwartzii	PSCH	
Other		
Cyst A	CYSA	Not included in statistical analyses

Table 4. Environemental parameters included in the statistical analyses corresponding to the database sampling sites: summer and winter temperatures (S_SST and W_SST; °C), summer and winter salinities (S_SSS and W_SSS), summer, winter and annual primary productivity estimated by moDIS and CZCS programs ($gC \cdot m^{-2} \cdot yr^{-1}$), the water depth (m) and the distance inshore-offshore (km).

					Summer Produc.		Winter Produc.		Annual Produc.			
Sites	S_SST	W_SST	S_SSS	W_SSS	MODIS	ANTOINE	MODIS	ANTOINE	MODIS	ANTOINE	Water Depth (m)	Distance inshore-offshore
1	28.39	19.16	34.94	34.82	50.01	91.70	163.05	98.06	411.42	390.14	38.80	1.36
2	28.12	19.13	34.91	34.72	50.01	81.66	163.05	93.74	411.42	355.78	334.00	11.89
3	28.33	19.22	34.91	34.78	34.70	72.44	139.73	91.03	308.08	330.42	282.00	8.28
4	28.66	19.26	34.91	34.79	34.70	72.44	139.73	91.03	308.08	330.42	888.00	4.18
5	28.55	19.24	34.91	34.81	50.01	72.44	139.73	91.03	308.08	330.42	34.00	9.34
6	28.41	19.19	34.91	34.79	50.01	76.99	163.05	93.80	411.42	346.51	401.00	11.71
7	28.68	19.23	34.94	34.87	34.70	84.13	163.05	97.65	411.42	373.16	29.50	2.14
8	28.41	19.15	34.91	34.79	50.01	73.81	163.05	92.19	411.42	334.83	395.00	7.22
9	28.60	19.19	34.91	34.81	34.70	69.56	139.73	89.51	308.08	319.87	348.00	19.84
10	28.60	19.23	34.91	34.79	34.70	69.56	139.73	89.51	308.08	319.87	850.00	11.52
11	28.57	19.12	34.91	34.86	50.01	70.56	163.05	92.05	411.42	329.04	312.00	10.97
12	28.41	19.11	34.91	34.85	50.01	70.56	163.05	92.05	411.42	329.04	324.00	4.56
13	29.12	21.75	34.74	34.82	90.93	44.02	203.32	52.48	583.13	200.31	61.40	8.94
14	29.45	21.65	34.74	34.83	90.93	51.11	203.32	60.43	583.13	232.38	60.70	14.15
15	29.45	21.90	34.74	34.83	90.93	48.27	203.32	56.29	583.13	213.74	207.30	35.87
16	29.44	21.94	34.69	34.84	90.93	50.51	203.32	56.55	583.13	217.86	366.00	43.73
17	29.69	22.67	34.58	34.71	61.92	56.02	134.10	58.54	476.16	234.54	51.20	38.20
18	29.69	22.80	34.58	34.71	61.92	57.48	134.10	58.21	476.16	237.40	74.00	47.90
19	29.80	22.80	34.58	34.65	61.92	85.27	134.10	61.39	476.16	295.16	36.60	12.90
20	30.28	22.59	34.39	34.55	56.33	90.93	154.86	68.35	491.02	333.37	60.00	18.60
21	29.85	23.83	34.28	34.57	50.75	74.13	175.62	60.59	505.89	283.80	418.10	58.30
22	29.84	24.05	34.28	34.55	50.75	51.93	175.62	52.03	505.89	238.28	422.80	36.00
23	29.65	24.11	34.28	34.53	50.75	52.22	175.62	51.83	380.88	235.16	71.60	8.30
24	29.64	23.97	34.28	34.58	50.75	43.78	175.62	43.39	505.89	229.24	1687.00	7.00
25	29.58	23.91	34.28	34.56	52.11	41.04	173.20	43.74	499.59	193.52	1127.00	3.60
26	30.35	23.36	34.28	34.55	53.34	47.51	171.48	49.45	495.14	217.76	278.00	1.35
27	29.69	24.17	34.28	34.54	35.43	46.45	132.48	55.46	325.72	243.44	79.40	1.40
28	29.49	24.22	34.28	34.54	35.43	45.93	132.48	58.05	325.72	252.36	204.80	13.00
29	29.29	24.50	34.17	34.47	35.43	43.46	132.48	66.99	325.72	276.94	1126.00	34.20
30	29.32	24.42	34.19	34.47	35.43	43.16	132.48	71.72	325.72	282.91	615.00	18.60
31	29.31	24.40	34.28	34.53	41.11	42.50	114.87	74.89	345.83	289.16	77.20	5.30

					Summer Produc.		Winter Produc.		Annual Produc.			
Sites	S_SST	W_SST	S_SSS	W_SSS	MODIS	ANTOINE	MODIS	ANTOINE	MODIS	ANTOINE	Water Depth (m)	Distance inshore-offshore
32	29.46	25.14	34.06	33.98	34.52	42.71	68.82	57.75	209.23	251.00	587.60	8.43
33	29.46	25.55	34.03	34.34	34.52	40.84	68.82	52.58	209.23	226.10	67.40	0.66
34	29.44	25.52	34.52	34.31	34.52	43.33	68.82	53.28	209.23	235.08	228.50	6.68
35	29.48	25.53	34.52	34.31	34.52	43.33	68.82	53.28	209.23	235.08	551.80	11.35
36	29.46	25.60	34.52	34.31	34.52	40.35	68.82	49.39	209.23	216.55	1188.00	23.82
37	29.50	26.15	33.85	34.35	39.24	41.39	74.21	52.30	255.58	210.84	61.30	4.10
38	29.49	26.16	33.85	34.35	39.24	41.39	74.22	52.30	255.58	210.84	102.60	7.50
39	29.55	26.50	33.85	33.76	39.24	46.22	74.22	59.44	255.58	232.17	96.60	2.70
40	29.51	26.40	33.85	33.76	39.24	46.22	74.22	59.44	255.58	232.17	191.20	8.90
41	29.40	26.92	33.85	33.93	34.10	47.69	47.96	55.39	178.67	219.55	58.50	1.80
42	29.39	26.90	33.85	33.87	34.10	47.69	47.96	55.40	178.67	219.55	362.30	9.10
43	29.64	27.19	33.60	34.18	35.85	43.46	57.44	40.22	198.65	188.28	713.90	29.40
44	29.61	27.18	33.60	34.18	35.85	43.46	57.44	40.22	198.65	188.28	428.90	23.20
45	29.63	27.13	33.47	34.18	35.85	44.03	57.44	42.61	198.65	198.89	92.80	8.10
46	29.76	27.12	33.14	34.18	35.85	47.60	57.44	40.67	198.65	202.28	36.50	5.40
47	29.84	27.43	33.14	34.36	35.85	44.81	57.44	38.80	198.65	181.53	63.40	4.29
48	29.91	27.45	33.14	34.36	35.85	44.81	57.44	38.80	198.65	181.53	173.40	10.36
49	29.83	27.45	33.14	34.36	31.15	44.81	31.12	38.80	127.92	181.53	883.10	14.65
50	29.85	27.37	33.14	34.36	31.15	43.90	31.12	39.62	127.92	181.09	995.10	25.80
51	29.68	27.43	33.14	34.28	34.07	47.62	41.42	46.50	157.67	199.45	153.00	5.90
52	29.64	27.40	33.14	34.26	34.07	47.62	41.42	46.50	157.67	199.45	73.00	3.20
53	29.66	27.41	33.14	34.08	41.23	47.15	58.09	43.82	188.81	187.75	58.90	1.50
54	29.58	27.59	33.14	33.93	41.23	54.65	58.09	45.76	188.81	195.65	24.00	0.20
55	29.55	27.58	33.14	33.97	41.23	54.65	58.09	45.77	188.81	195.67	79.80	2.10
56	29.62	27.56	33.14	33.98	41.23	47.15	58.09	43.82	188.81	187.75	241.40	9.45
57	29.69	27.75	33.14	33.95	41.23	47.82	58.09	49.37	188.81	190.91	51.50	5.07
58	29.96	27.88	34.00	34.00	41.84	56.55	64.24	45.64	201.60	213.40	72.60	2.00
59	29.72	27.90	34.00	34.01	41.84	56.29	64.24	47.30	201.60	219.07	70.10	1.00
60	29.42	26.31	33.53	34.20	46.99	71.78	160.02	75.08	384.29	342.75	700.00	27.70
61	29.43	26.29	33.53	34.20	46.99	76.24	160.02	76.48	384.29	354.74	225.00	17.50
62	29.34	26.35	33.69	34.19	46.64	77.32	143.18	78.75	349.88	362.24	290.00	23.90
63	29.28	26.39	33.69	34.18	46.64	74.40	143.18	77.19	349.88	352.68	600.00	32.40
64	29.35	26.37	33.69	34.21	46.64	74.40	143.18	77.19	349.88	352.68	1025.00	43.50
65	29.26	26.20	33.92	34.27	46.78	71.83	166.51	75.21	345.00	342.09	1050.00	81.20
66	29.33	26.38	33.69	34.22	46.64	74.66	143.18	78.24	349.88	355.78	280.00	59.70
67	29.24	26.38	33.69	34.19	46.64	75.55	143.18	79.07	349.88	359.55	166.00	45.10
68	29.33	26.62	33.64	34.06	46.64	74.65	143.18	82.18	349.88	367.54	67.50	21.60
69	29.41	26.69	33.64	33.94	46.64	69.03	143.18	78.06	349.88	338.11	68.00	21.90

Sites	S_SST	W_SST	S_SSS	W_SSS	Summer Produc.		Winter Produc.		Annual Produc.		Water Depth (m)	Distance inshore-offshore
					MODIS	ANTOINE	MODIS	ANTOINE	MODIS	ANTOINE		
70	29.32	26.38	33.64	34.18	46.64	68.88	143.18	76.17	349.88	331.02	240.00	45.60
71	29.24	26.40	33.64	34.24	46.64	67.53	143.18	75.09	349.88	326.64	187.00	68.50
72	29.21	26.29	33.92	34.32	46.78	64.37	166.51	71.67	345.00	311.42	230.00	91.00
73	29.41	26.04	33.92	34.35	46.11	55.46	133.80	65.38	296.09	275.80	303.00	109.00
74	29.27	26.43	34.00	34.27	46.78	60.33	166.51	68.97	345.00	291.38	234.00	85.80
75	29.25	26.48	33.64	34.23	46.64	63.80	143.18	72.83	349.88	308.57	230.00	64.70
76	29.15	26.39	34.00	34.48	46.78	58.36	166.51	68.18	345.00	285.97	227.00	96.20
77	29.41	26.67	33.64	33.88	46.64	64.45	143.18	75.33	349.88	320.17	52.00	20.20
78	29.38	26.29	33.92	33.98	45.86	61.04	143.18	70.30	258.66	266.03	95.00	37.40
79	29.29	26.81	33.64	33.78	44.61	54.43	70.02	65.14	206.18	269.92	242.00	55.20
80	29.56	26.71	33.64	33.97	45.00	48.39	85.32	60.03	219.18	246.15	283.00	108.00
81	29.55	26.85	33.64	33.86	45.00	39.12	85.32	50.41	219.18	192.85	245.00	93.00
82	29.40	26.95	33.64	33.76	45.00	39.92	85.32	50.51	219.18	193.85	224.00	72.60
83	29.39	26.88	33.64	33.78	45.00	39.03	85.32	49.38	219.18	192.01	213.00	65.50
84	29.60	26.78	33.68	33.96	45.24	53.00	84.13	63.07	217.16	228.69	110.00	44.50
85	29.60	26.63	33.69	33.96	45.50	57.12	143.18	66.94	214.55	255.08	47.00	24.40
86	29.37	27.46	33.73	33.92	46.69	36.38	85.32	42.77	219.18	141.46	60.00	41.30
87	29.68	27.24	33.78	33.67	45.00	33.71	85.32	38.82	219.18	145.83	180.00	23.00
88	29.94	27.20	33.78	33.56	45.00	36.41	85.32	42.07	219.18	158.60	187.00	74.70
89	29.95	27.66	33.78	33.48	56.40	41.87	46.35	39.44	190.58	157.39	87.00	45.80
90	29.55	27.69	33.78	33.49	56.40	41.87	46.35	39.44	190.58	157.39	45.00	37.80
91	29.40	27.75	33.77	33.51	55.78	43.51	46.35	40.42	190.58	165.06	35.00	22.30
92	29.40	27.76	33.78	33.49	56.40	45.89	46.35	40.48	190.58	196.55	44.00	28.90
93	30.34	28.11	33.77	33.45	55.18	43.85	46.35	42.85	190.58	223.72	88.00	46.40
94	29.95	27.73	33.78	33.45	56.40	43.74	46.35	44.12	190.58	176.16	258.00	67.40
95	29.78	27.46	33.56	33.58	45.00	38.68	85.32	46.23	219.18	177.30	220.00	88.00

4. RESULTS

4.1 Geochemical data

Throughout the study area, percentages of total organic carbon (TOC) in sediment are relatively high and range from 0.25% to 5.08%. TOC shows higher values with increased distance to the shore and depth (Figure 3B-C). Elemental analyses performed on surface sediments show C:N ratios ranging from 5.35 to 15.44, except for station 59 which has a value of 22.74 (Figure 3A). Carbon isotope signatures ($\delta^{13}C_{org}$) increase with the distance to the shore and depth, and are of the order of -21.02% to -25.91%, with most of the values comprised between -21 % and -23.5 % (Figure 3A-B-C) (Table 5). Both TOC and $\delta^{13}C$ indicate higher contribution of marine fluxes offshore likely related to lesser terrigenous inputs and lower sedimentation rates.

4.2 Palynomorph assemblages

Palynomorph assemblages are characterized by terrestrial (pollen grains) and marine components (foraminifer organic linings and dinocysts) with higher concentrations of marine microfossils throughout the study area (Figure 4).

Dinocyst concentrations calculated from dry weight of sediment are highly variable (from 66 to 55 620 cysts·g^{-1}) and follow a latitudinal gradient with highest values in the Northern part of the study area and a decreasing trend toward the Tehuantepec Gulf (Figure 5, Tables 6-7). Concentrations in our study area are high in comparison with the concentrations observed in the coastal zones of North America north of 40°N (e.g. Radi et al., 2007; Pospelova et al., 2008) and reflect high planktonic productivity. Otherwise, observations from sites located in Tehuantepec Gulf are consistent with the results of Vásquez-Bedoya et al. (2008).

Concentrations of organic linings are of the order of ~ 65 to 34 000 linings·g^{-1} (see table 6-7). These values are high comparatively to those reported from other studies (e.g. Pospelova et al., 2008; Thibodeau et al., 2006; Hamel et al., 2002). Since foraminifer organic linings represent a fragmentary picture of the biocenoses, their abundant content suggests very high benthic productivity. Analyses of benthic foraminifera shells versus linings are also used as

proxy for carbonate dissolution in sediments (de Vernal et al., 1992). In La Paz Bay, higher lining concentrations contrast with a low number of foraminifer shells, reflecting dissolution processes in sediments. On the contrary, shell vs. lining ratios in the Northern part of Tehuantepec Gulf suggest that calcium carbonate in sediments from that region are well-preserved (e.g. Kielt, 2006).

Pollen grain concentrations are highly variable with values ranging from ~216 to 64 736 pollens·g^{-1} (see tables 6-7). Low terrestrial palynomorph concentrations were recorded in La Paz Bay and along the Mexican margin, whereas the Northern part of Tehuantepec Gulf shows maximal values.

Ratios of dinocyst to pollen grains are often used as "continentallity" index (e.g., de Vernal and Giroux, 1991). Values are comprised between 0.05 and 3.29 along the Mexican margin and Tehuantepec Gulf and the lowest ratios are observed in the Northern part of Tehuantepec Gulf and at station 59 (0.05 and 0.07) (see tables 6-7). Sites from La Paz Bay show dominant dinocyst concentrations with ratios reaching up to 7.78.

4.3 Dinocyst assemblages

With a total of 34 taxa identified, dinocyst assemblages show a large diversity of dinocyst species, notably among heterotrophic ones (Figures 6-7). The abundance and good preservation of the observed Protoperidinium and *Echinidinium* cysts, in spite of their extreme sensitivity to oxidation processes (Zonneveld et al., 2001) indicate a good preservation of organic matter and dinocysts in sediment.

Bitectatodinium spongium and *Brigantedinium* spp. are abundant all along the coast and correspond together to more than 40% of the assemblages. Heterotrophic taxa are likely to dominate in upwelling zones with *Brigantedinium* spp., *Selenopemphix quanta*, *Polykrikos kofoidii* and *Echinidinium* species. In addition, the upwelling area of Tehuantepec Gulf is marked by a high occurrence of the phototrophic taxon *Polysphaeridium zoharyi*. In opposition, most phototrophic taxa including *Bitectatodinium spongium* and *Spiniferites* spp. principally occur in regions which are not under the influence of upwelling.

Several sites are characterized by the presence of cysts of harmful taxa such as *Polysphaeridium zoharyi*, cyst of *Gymnodinium catenatum* and *Lingulodinium machaerophorum*. While the main zone of occurrence of *P. zoharyi* is observed in the Northern part of Tehuantepec Gulf (Figure 8A), the distribution of *L. machaerophorum* is scattered among the study sites, notably between Mazatlán and Puerto Vallarta (Figure 8B). Due to their poor state of preservation in several slides, cysts of *Gymnodinium catenatum* were not counted. This species appears fragmented most of the time, which makes the quantification of its occurrence in sediment difficult (Plate 1). *G. catenatum* has been reported in bloom events implicating massive shrimp mortalities along the western Mexican coast (Alonso-Rodríguez, 2003). Unfortunately, the poor preservation of the cysts in sediments does not permit their use for analysing dinocyst distribution in relation to hydrographical conditions and therefore identifying parameters favourable to HABs related to *G. catenatum* blooms.

4.2 Statistical analyses

Redundancy analysis further provides insight into the relationship between dinocyst distribution and environmental parameters. The first two axes explain respectively 43.7% and 29.4% of the total variance. Although the absence of a strong correlation between individual taxa and the first two axes, some hydrographical parameters are likely to play a role in the geographical distribution of the dinocyst assemblages (Tables 8-9-10). The nearshore-offshore gradient is strongly linked to the first axis (R = 0.7336), whereas annual, winter and summer productivity and winter salinity correlate with axis 2 (R= 0.689, 0.569, 0.616 and 0.616). *Echinidinium transparantum* is in the negative domain of axis 1. Otherwise, axis 2 shows a relation with the relative abundance of heterotrophic taxa (R^2 = 0.75394) (Figure 9) and is characterized by an opposition between *Spiniferites delicatus* on the positive side and heterotrophic taxa in the negative side of the ordination (Figure 10).

The sample scores for axes 1 and 2 in the ordination diagram illustrate different regional groupings. Here, four assemblages are well defined and the similarities between assemblages from sites located in upwelling areas are clearly shown (Figures 11-12):

- Assemblage 1 corresponds to the upwelling zone of La Paz Bay. This assemblage is characterized by high dinocyst concentrations and its composition is dominated by heterotrophic-related taxa such as *Polykrikos kofoidii*, *Echinidinium aculeatum*, *Echinidinium granulatum* and *Brigantedinium* spp.

- Assemblage 2 represents the coastal zone comprised between the California Bay and Tehuantepec Bay where human activities are developing rapidly. Total cyst concentrations follow a decreasing trend, with highest values between Mazatlán and Manzanillo and lower values towards the Tehuantepec Gulf. Heterotrophic species *Polykrikos kofoidii*, *Echinidinium* spp. and *Brigantedinium* spp. largely dominate. Moreover, *Bitectatodinium spongium* is present in higher proportions.

- Assemblage 3 is restricted to the Northern part of the Tehuantepec Gulf, where seasonal upwelling results in high primary productivity. This area is however marked by low dinocyst concentrations, high *Polysphaeridium zoharyi* occurrence and relatively high proportions of *Spiniferites* spp.

- Assemblage 4 is associated to the Southern part of the Tehuantepec Gulf, which is not under the influence of upwelling and which is characterized by a low productivity. Dinocyst concentrations and the ratios of heterotrophic to autotrophic species show the lowest values. This assemblage is dominated by *Bitectatodinium spongium*, *Spiniferites* spp. and *Brigantedinium* spp. Finally, *Spiniferites delicatus* exhibits in this zone its greatest relative abundance.

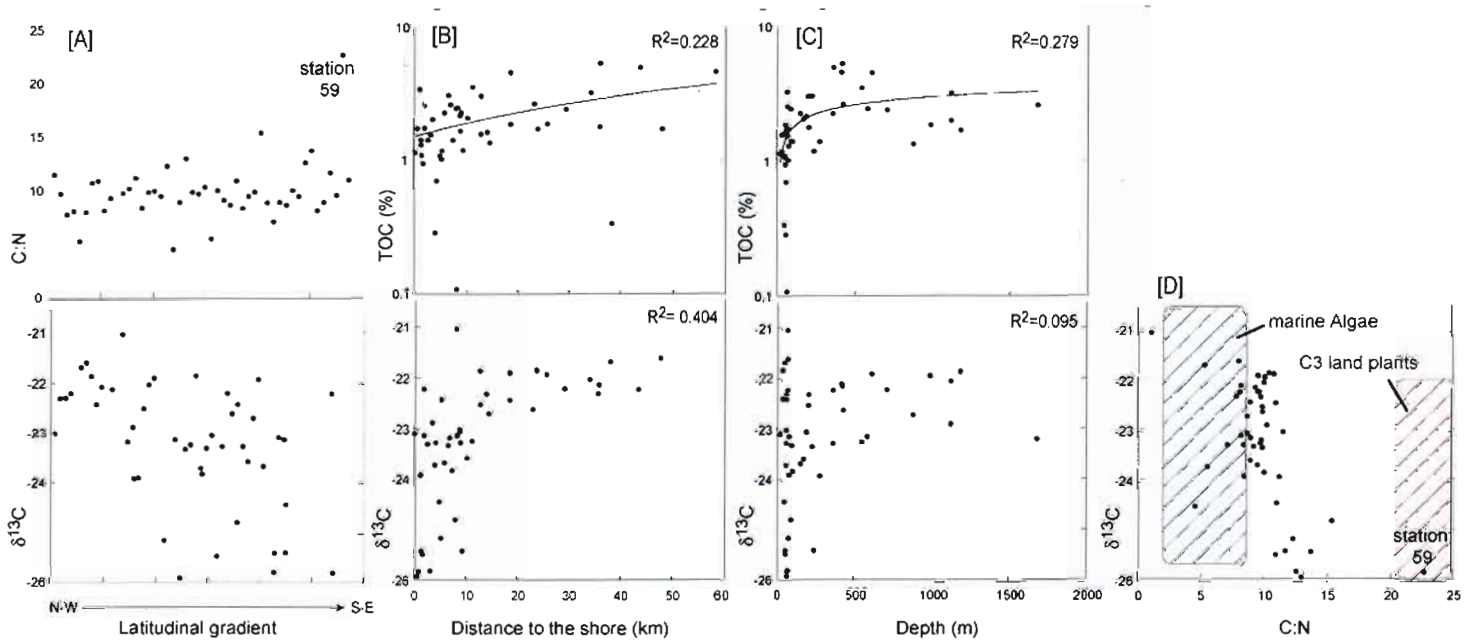

Figure 3. Spatial distribution of C:N, TOC (%) and $\delta^{13}C$ of sediments from the Mexican margin. (A) C:N ratios and isotopic composition of organic carbon ($\delta^{13}C$) vs latitudinal gradient, (B) Percentages of total organic carbon (TOC) and $\delta^{13}C$ vs the distance to the shore, (C) TOC and $\delta^{13}C$ vs depth, (D) $\delta^{13}C$ vs C:N ratios.
Data are not available for La Paz Bay and Tehuantepec Gulf.

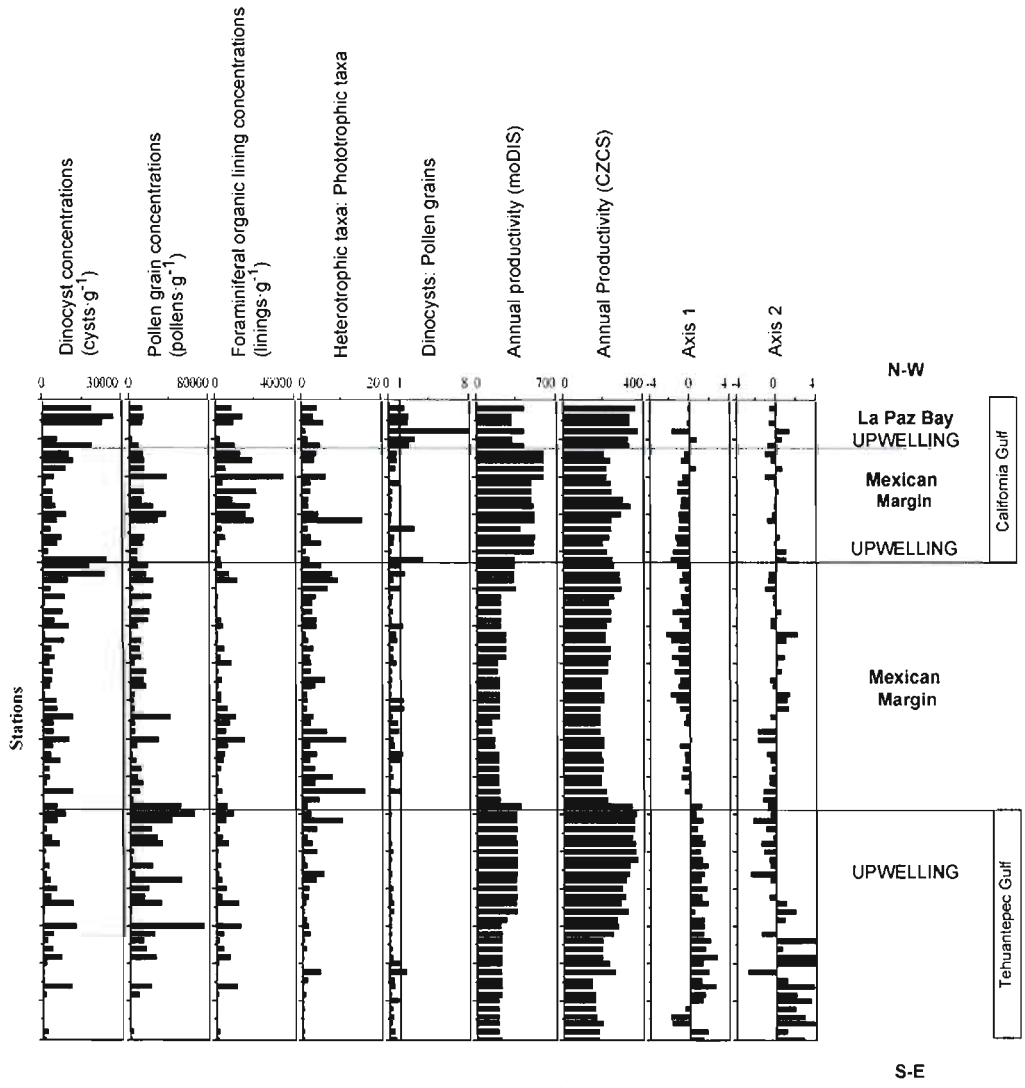

Figure 4. Dinocyst concentrations (cysts·g^{-1}), pollen grain concentrations (grains·g^{-1}), foraminifer organic lining concentrations (linings·g^{-1}), heterotrophic to phototrophic taxa ratios, dinocysts to pollen grains ratios, annual productivity estimated by moDIS program, annual productivity estimated by CZCS program and sample scores of axes 1 and 2 from redundancy analysis.

Table 5. Elemental and isotopic analyses, depth and distance to the shore of surface-sediment samples of this study.

Sites	TC	TIC	TOC	TN	C:N	$\delta^{13}C$	Depth	Distance to the shore
	(%)	(%)	(%)	(%)			(m)	(km)
13	2.34	0.66	1.68	0.17	11.55	-	61.40	8.94
14	2.67	1.03	1.65	0.20	9.76	-	60.70	14.15
15	2.91	1.09	1.82	0.27	7.83	-	207.30	35.87
16	7.26	2.18	5.08	0.73	8.11	-	366.00	43.73
17	2.96	2.62	0.34	0.07	5.35	-	51.20	38.20
18	3.92	2.17	1.75	0.25	8.02	-	74.00	47.90
19	1.83	0.25	1.59	0.17	10.78	-	36.60	12.90
20	2.45	0.56	1.89	0.20	10.94	-	60.00	18.60
21	6.49	1.80	4.69	0.67	8.19	-	418.10	58.30
22	6.20	0.78	5.43	0.68	9.33	-	422.80	36.00
23	9.61	9.50	0.11	0.11	1.13	-	71.60	8.30
24	3.17	0.52	2.65	0.32	9.81	-	1687.00	7.00
25	2.42	0.37	2.05	0.23	10.25	-	1127.00	3.60
26	1.65	0.22	1.43	0.15	11.24	-	278.00	1.35
27	2.06	0.74	1.32	0.18	8.46	-	79.40	1.40
28	3.43	0.36	3.08	0.36	9.88	-	204.80	13.00
29	3.67	0.40	3.27	0.38	10.03	-	1126.00	34.20
30	5.44	0.80	4.63	0.57	9.54	-	615.00	18.60
31	1.63	0.60	1.03	0.10	12.33	-	77.20	5.30
32	3.40	0.89	2.51	0.33	8.96	-	587.60	8.43
33	2.00	0.25	1.75	0.16	13.03	-	67.40	0.66
34	3.74	0.63	3.11	0.37	9.91	-	228.50	6.68
35	4.47	0.88	3.60	0.43	9.75	-	551.80	11.35
36	1.93	0.19	1.74	0.19	10.41	-	1188.00	23.82
37	1.55	1.26	0.29	0.06	5.58	-	61.30	4.10
38	1.97	0.54	1.43	0.17	10.06	-	102.60	7.50
39	2.22	0.79	1.43	0.18	9.18	-	96.60	2.70
40	2.95	0.75	2.20	0.29	8.70	-	191.20	8.90
41	1.42	0.46	0.96	0.10	10.98	-	58.50	1.80
42	3.40	1.10	2.31	0.32	8.42	-	362.30	9.10
43	2.99	0.54	2.46	0.30	9.51	-	713.90	29.40
44	3.12	0.41	2.71	0.32	9.90	-	428.90	23.20
45	4.48	2.00	2.49	0.19	15.44	-	92.80	8.10
46	2.21	1.02	1.19	0.15	8.93	-	36.50	5.40
47	1.85	1.14	0.71	0.12	7.15	-	63.40	4.29
48	2.89	0.79	2.10	0.27	8.96	-	173.40	10.36
49	2.01	0.64	1.37	0.18	8.71	-	883.10	14.65
50	2.25	0.35	1.90	0.22	10.08	-	995.10	25.80
51	3.13	0.82	2.31	0.28	9.50	-	153.00	5.90
52	1.99	0.42	1.57	0.14	12.63	-	73.00	3.20
53	1.71	0.62	1.10	0.09	13.78	-	58.90	1.50
54	1.67	0.58	1.09	0.11	11.07	-	51.50	5.07
55	1.74	0.59	1.15	0.16	8.21	-	24.00	0.20
56	2.43	0.68	1.75	0.23	8.97	-	79.80	2.10
57	1.59	0.38	1.21	0.12	11.73	-	241.40	9.45
58	3.09	0.49	2.60	0.31	9.64	-	72.60	2.00
59	4.88	1.54	3.34	0.17	22.74	-	70.10	1.00

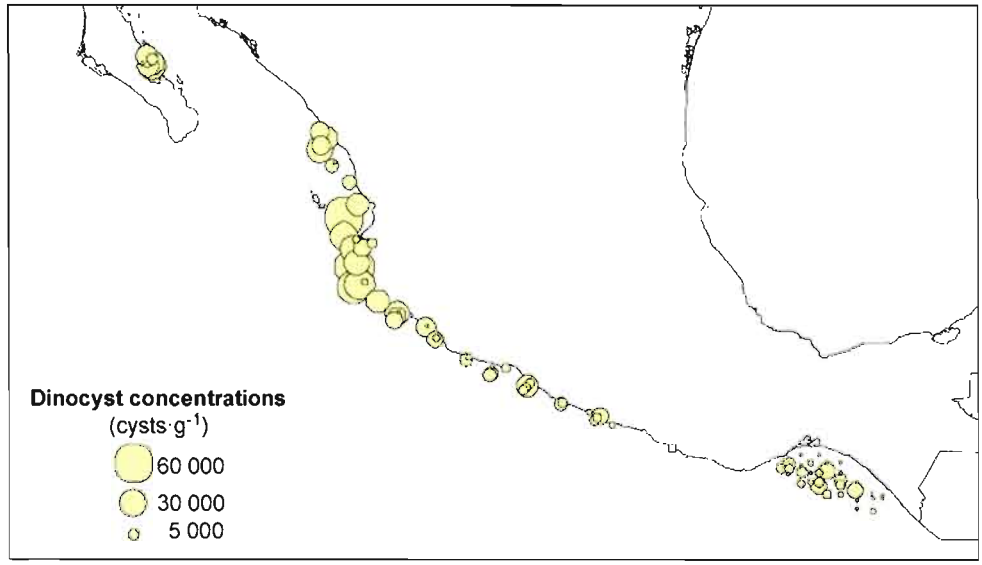

Figure 5. Distribution of total dinoflagellate cyst concentrations (cysts·g^{-1}).

Table 6. Terrestrial and marine palynomorph concentrations of surface sediment sampled in this study: dinocyst, pollen grain and foraminiferal organic lining concentrations, ratios of heterotrophic to phototrophic dinocyst taxa and dinocysts to pollen grains ratios.

Sites	Dinocyst concentrations (cysts·g^{-1})	Pollen grains concentrations (grains·g^{-1})	Foraminiferal organic lining concentrations (linings·g^{-1})	Heterotrophic dinocysts / Phototrophic dinocysts	Dinocysts / Pollen grains
13	9964.33	13626.73	12197.71	3.51	0.73
14	11333.79	14896.55	18285.34	3.00	0.76
15	8634.81	14616.71	5011.44	0.32	0.59
16	4220.04	37264.01	33982.90	5.95	0.11
17	1121.47	1255.85	3353.95	2.27	0.89
18	3674.21	13802.27	20353.09	1.99	0.27
19	3465.48	12329.22	8219.48	1.49	0.28
20	4836.45	23193.05	16935.69	1.59	0.21
21	8623.67	36958.16	15185.78	4.03	0.23
22	5352.62	28605.53	19037.47	14.84	0.19
23	2818.87	1160.09	2880.22	1.42	2.43
24	6932.89	14830.28	4617.81	2.20	0.47
25	5368.42	12880.05	1708.58	4.61	0.42
26	1871.12	7785.07	519.94	0.83	0.24
27	23711.91	7196.85	2294.65	1.85	3.29
28	17140.74	17660.82	2999.01	4.62	0.97
29	23058.09	15933.50	6373.40	7.44	1.45
30	9306.37	22899.69	10836.46	8.78	0.41
31	2894.07	2663.32	620.98	6.31	1.09
32	8111.63	20913.29	806.51	3.37	0.39
33	575.94	2268.33	369.87	2.56	0.25
34	7211.68	19376.25	340.88	2.45	0.37
35	4387.05	17886.93	2285.61	3.43	0.25
36	9725.10	7539.14	3464.18	3.42	1.29
37	650.41	1066.63	874.10	0.66	0.61
38	7620.37	10746.84	920.83	1.32	0.71
39	3051.52	9134.84	3913.61	2.63	0.33
40	4181.18	10997.89	2140.98	1.82	0.38
41	2421.42	4032.45	7655.15	2.21	0.60
42	3644.67	16064.29	1254.60	2.10	0.23
43	3347.18	13147.62	2653.47	5.64	0.25
44	2511.64	15830.39	1276.32	3.22	0.16
45	682.11	5198.83	2352.93	1.05	0.13
46	4971.98	3734.91	2307.23	1.25	1.33
47	5279.66	3949.96	5502.99	1.01	1.34
48	11019.26	40754.35	9979.83	2.63	0.27
49	3759.32	5047.80	6720.61	1.97	0.74
50	3825.11	4675.47	4567.08	6.05	0.82
51	9868.21	29150.34	14625.55	10.85	0.34
52	3468.83	6946.60	5801.49	1.80	0.50
53	2792.90	2298.76	4371.49	3.56	1.21
54	1352.64	12372.23	717.50	3.12	0.11
55	6227.15	6425.20	3722.73	1.91	0.97
56	2138.04	10873.48	1979.48	2.96	0.20
57	2369.37	7266.28	783.03	7.37	0.33
58	11028.93	9476.50	2876.64	15.59	1.16
59	220.01	3191.09	554.47	4.09	0.07

Table 7. Terrestrial and marine palynomorph concentrations of surface sediment sampled in La Paz Bay and Tehuantepec Gulf (cf. Kielt, 2006): dinocyst, pollen grain and foraminiferal organic lining concentrations, ratios of heterotrophic to phototrophic dinocyst taxa and dinocysts to pollen grains ratios.

Sites	Dinocyst concentrations (cyst·g^{-1})	Pollen grains concentrations (grains·g^{-1})	Foraminiferal organic lining concentrations (linings·g^{-1})	Heterotrophic dinocysts / Phototrophic dinocysts	Dinocysts / Pollen grains
1	-	-	-	2.26	-
2	18525.91	12712.33	7929.47	3.66	1.46
3	26606.59	14284.44	13344.79	2.81	1.86
4	-	-	-	4.80	-
5	22260.84	12548.97	9016.81	5.28	1.77
6	-	-	-	4.32	-
7	232.98	29.94	203.03	0.83	7.78
8	-	-	-	8.33	-
9	5574.72	2236.00	2132.36	1.44	2.49
10	-	-	-	8.21	-
11	-	-	-	3.29	-
12	18340.93	9549.43	9612.37	4.47	1.92
60	5337.89	51381.96	5337.89	1.28	0.10
61	-	-	-	10.17	-
62	8487.15	64736.62	8487.15	2.06	0.13
63	5123.32	42085.66	5123.32	10.06	0.12
64	1394.31	21209.47	1394.31	3.46	0.07
65	3153.54	27488.72	3153.54	1.27	0.11
66	5916.40	32353.34	5916.40	2.39	0.18
67	875.37	3324.48	875.37	3.44	0.26
68	382.43	1966.80	382.43	0.57	0.19
69	-	-	-	1.38	-
70	2063.49	22652.33	2063.49	1.03	0.09
71	1000.12	4350.75	1000.12	5.33	0.23
72	2635.98	51774.22	2635.98	3.40	0.05
73	-	-	-	1.29	-
74	4901.82	18375.34	4901.82	1.61	0.27
75	2873.30	14051.81	2873.30	1.45	0.20
76	11145.30	31803.34	11145.30	0.76	0.35
77	282.84	841.52	282.84	0.37	0.34
78	65.68	362.95	65.68	0.83	0.18
79	12243.00	74154.05	12243.00	1.35	0.17
80	3838.56	24282.33	3838.56	1.94	0.16
81	1538.86	13480.26	1538.86	0.35	0.11
82	3649.55	15927.49	3649.55	0.87	0.23
83	6849.32	26018.33	6849.32	0.18	0.26
84	1227.79	1178.19	1227.79	0.13	1.04
85	356.15	216.18	356.15	4.50	1.65
86	245.84	592.31	245.84	1.17	0.42
87	10636.56	20957.49	10636.56	0.26	0.51
88	1131.62	8612.65	1131.62	0.75	0.13
89	334.94	402.25	334.94	0.32	0.83
90	103.17	361.38	103.17	0.42	0.29
91	148.23	438.77	148.23	0.30	0.34
92	71.25	296.15	71.25	0.11	0.24
93	-	-	-	3.20	-
94	1723.38	3726.06	1723.38	0.42	0.46
95	1007.27	1655.08	1007.27	0.41	0.61

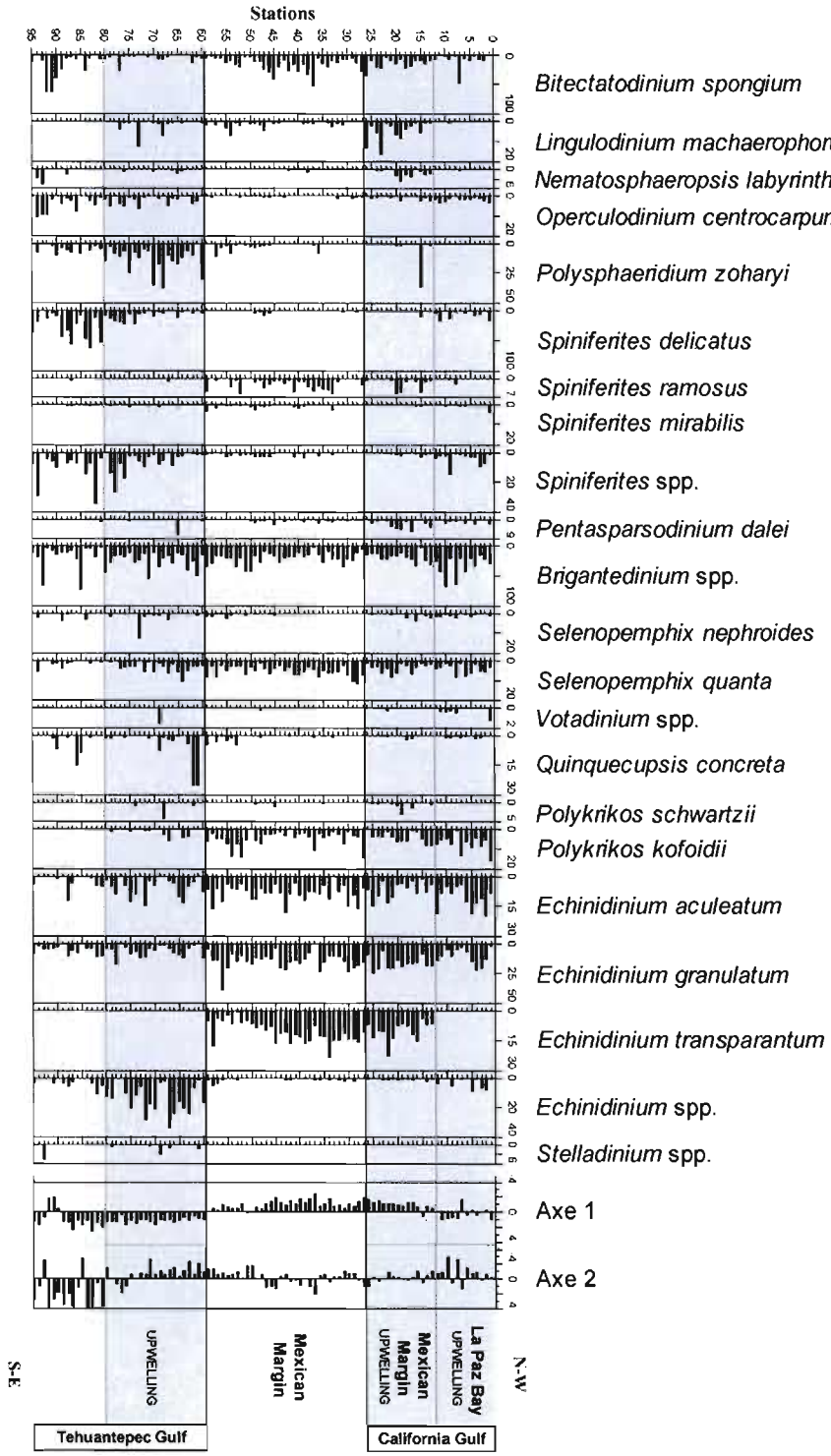

Figure 6. Percentages of the main dinocyst taxa and axes 1 and 2 scores from redundancy analysis.

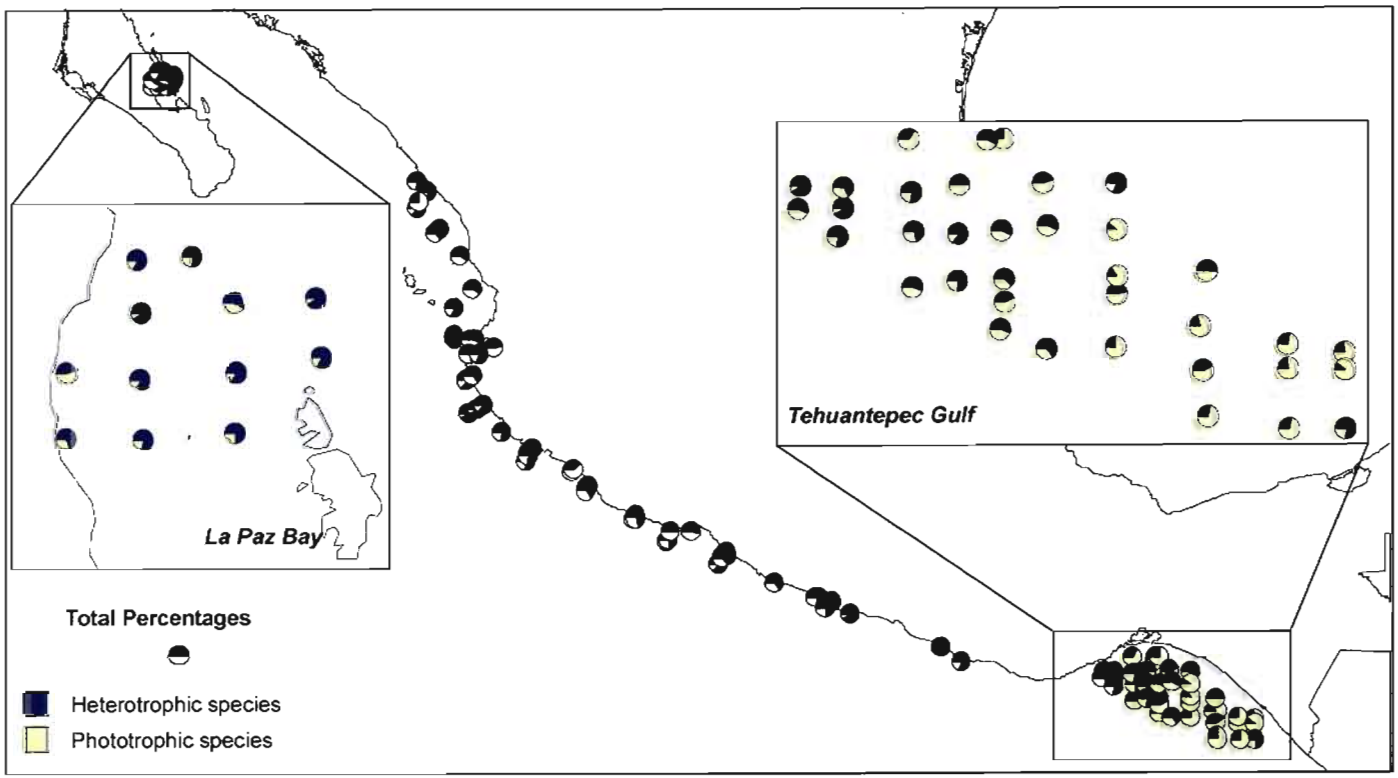

Figure 7. Distribution of the percentages of heterotrophic and phototrophic taxa in the assemblages of each station.

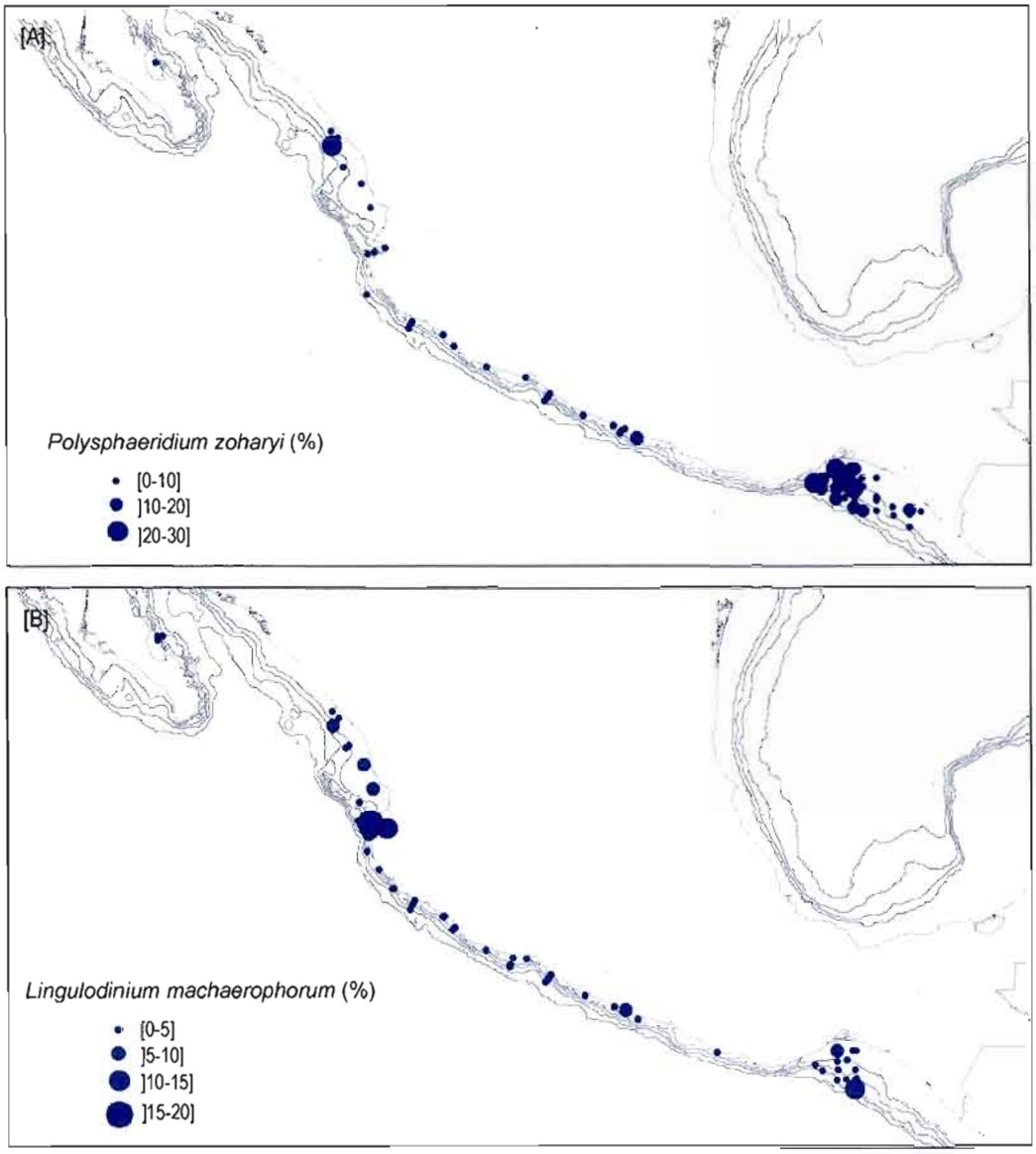

Figure 8. Maps showing the spatial extent and the percentages of potentially toxic species [A] *Polysphaeridium zoharyi*, [B] *Lingulodinium machaerophorum*. Isobath contours correspond to 200, 500, 1000 and 2000m.

Table 8. Scores of dinocyst taxa according to the two first axes of redundancy analysis.

Dinocyst taxa	Axis 1	Axis 2
Bitectatodinium spongium	-0.4562	0.3325
Lingulodinium machaerophorum	-0.2077	-0.1025
Nematosphaeropsis labyrinthus	-0.0673	-0.0139
Operculodinium centrocarpum	0.2992	0.2169
Polysphaeridium zoharyi	0.4556	-0.2184
Spiniferites delicatus	0.4778	0.5106
Spiniferites ramosus	-0.5402	-0.06
Spiniferites mirabilis	0.0833	0.1647
Spiniferites spp.	0.4684	0.3077
Pentapharsodinium dalei	-0.1564	-0.2204
Brigantedinium spp.	0.1781	-0.3584
Selenopemphix nephroides	0.2138	-0.0467
Selenopemphix quanta	-0.3298	-0.3014
Votadinium spp.	0.0377	-0.1363
Quinquecupsis concreta	0.1634	-0.1137
Polykrikos schwartzii	-0.117	-0.1636
Polykrikos kofoidii	-0.4213	-0.2948
Echinidinium aculeatum	-0.1812	-0.2216
Echinidinium granulatum	-0.3993	-0.08
Echinidinium transparantum	-0.7455	0.0329
Echinidinium spp.	0.5278	-0.2548
Stelladinium spp.	0.1082	-0.0626

Table 9. Coefficient of correlation between environmental parameters and the scores of the three first axes of redundancy analysis. Parameter abbreviations are: summer sea-surface temperature (S_SST), winter sea-surface temperature (W_WWT), summer sea-surface salinity (S_SSS), winter sea-surface salinity (W_SSS), summer productivity estimated by moDIS program (S_MODIS), summer productivity estimated by CZCS program (S_ANTOINE), winter productivity estimated by moDIS program (W_MODIS), winter productivity estimated by CZCS program (W_ANTOINE), annual productivity estimated by moDIS program (A_MODIS) and annual productivity estimated by CZCS program (A_ANTOINE). Bold numbers correspond to parameters which are best related to axes.

Environmental parameters	Axis 1	Axis 2	Axis 3
S_SST	-0.2338	0.3122	-0.2495
W_SST	0.1134	0.3631	-0.5015
S_SSS	-0.1453	-0.2024	0.4136
W_SSS	-0.2854	**-0.6164**	0.3689
S_MODIS	0.1149	0.0286	-0.1629
S_ ANTOINE	0.2852	**-0.6159**	-0.1166
W_MODIS	0.2236	-0.4375	0.0201
W_ANTOINE	0.3699	**-0.5686**	0.0871
A_MODIS	-0.0587	-0.3531	-0.0555
A_ANTOINE	0.3166	**-0.6891**	-0.1524
Depth	-0.0131	-0.367	0.3267
Nearshore-offshore gradient	**0.7336**	0.2507	-0.1471

Table 10. Correlation matrix resulting from redundancy analysis.

SPEC AX1	1.0000							
SPEC AX2	-.0256	1.0000						
SPEC AX3	.1806	-.2847	1.0000					
SPEC AX4	.0449	.1574	-.0497	1.0000				
ENVI AX1	.8421	.0000	.0000	.0000	1.0000			
ENVI AX2	.0000	.6549	.0000	.0000	.0000	1.0000		
ENVI AX3	.0000	.0000	.6140	.0000	.0000	.0000	1.0000	
ENVI AX4	.0000	.0000	.0000	.5072	.0000	.0000	.0000	1.0000
S_SST	-.1969	.2045	-.1532	.1035	-.2338	.3122	-.2495	.2041
W_SST	.0955	.2378	-.3079	.0784	.1134	.3631	-.5014	.1545
S_SSS	-.1224	-.1326	.2539	-.0308	-.1453	-.2024	.4136	-.0607
W_SSS	-.2403	-.4037	.2265	.0785	-.2854	-.6164	.3689	.1547
S_MODIS	.0967	.0187	-.1000	-.0291	.1149	.0286	-.1629	-.0574
S_ ANTOINE	.2402	-.4033	-.0716	-.0929	.2852	-.6159	-.1166	-.1832
W_MODIS	.1883	-.2865	.0123	.1167	.2236	-.4375	.0201	.2301
W_ANTOINE	.3115	-.3724	.0535	-.0956	.3699	-.5686	.0870	-.1885
A_MODIS	-.0494	-.2312	-.0341	.1194	-.0587	-.3531	-.0555	.2355
A_ANTOINE	.2666	-.4513	-.0936	-.0473	.3166	-.6891	-.1524	-.0933
Water Depth	-.0110	-.2403	.2006	.3032	-.0131	-.3670	.3267	.5978
Nearshore-offshore gradient	.6178	.1642	-.0903	.2119	.7336	.2507	-.1470	.4179
	SPEC AX1	SPEC AX2	SPEC AX3	SPEC AX4	ENVI AX1	ENVI AX2	ENVI AX3	ENVI AX4

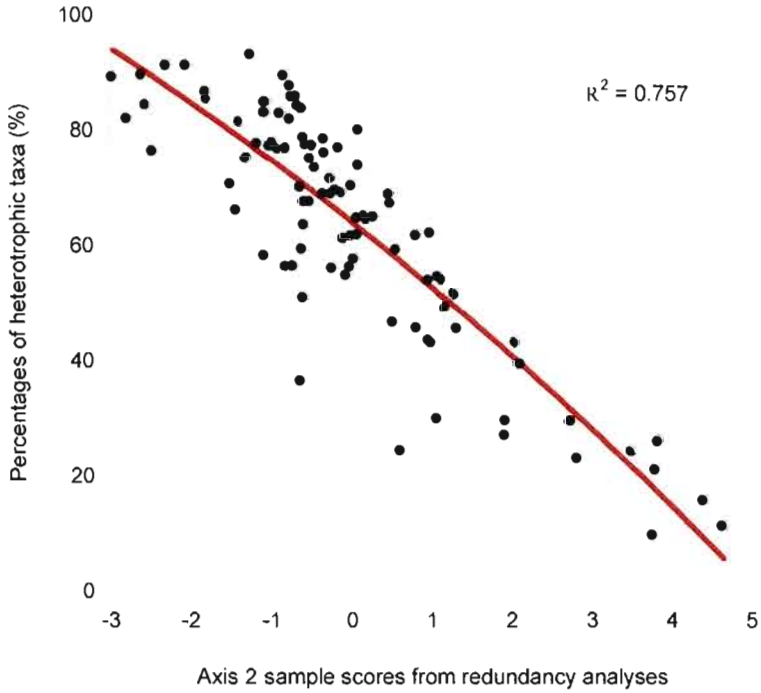

Figure 9. Percentages of heterotrophic taxa vs axis 2 sample scores from redundancy analyses which represent 29.4% of the variance. Note that axis 2 is negatively correlated with productivity (R^2=0.689 for annual productivity).

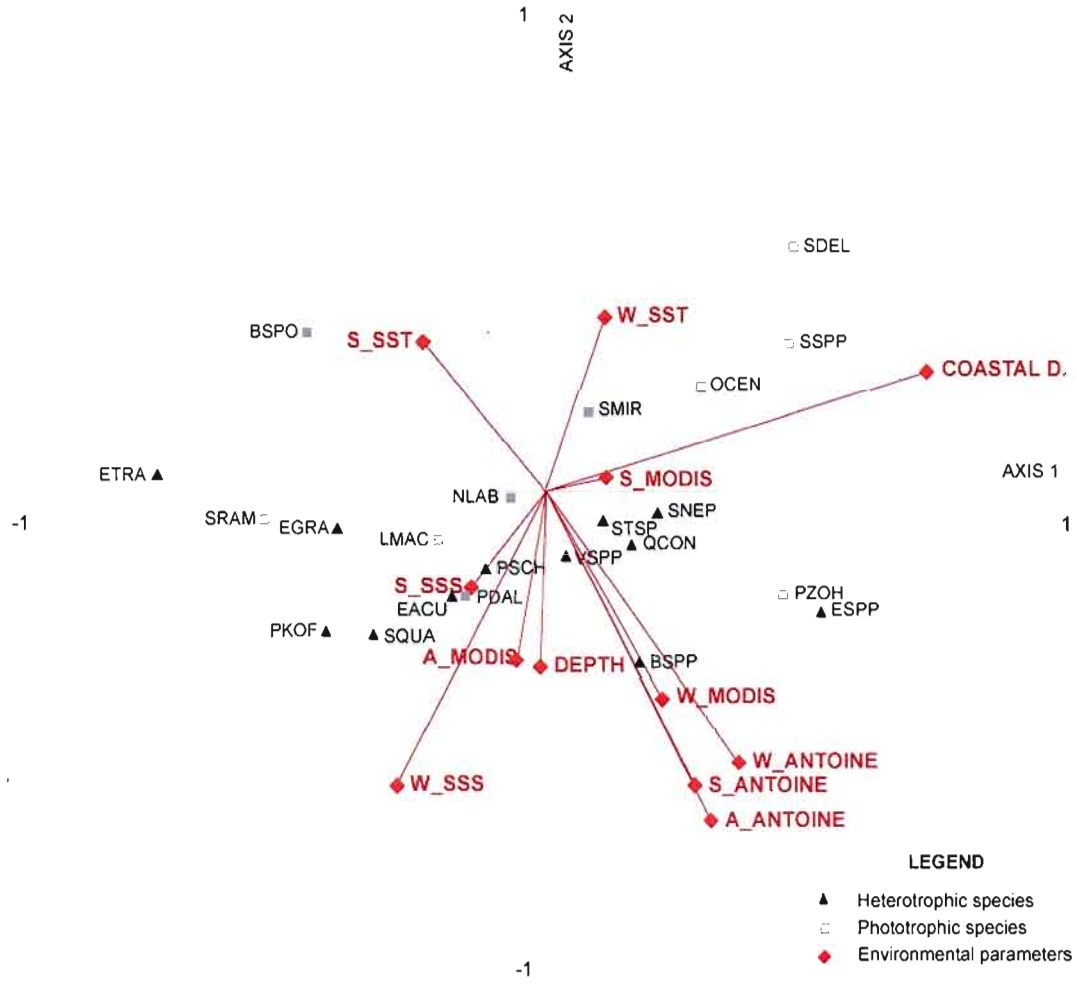

Axes	1	2	3	4	Total variance
Eigen values	.176	.118	.044	.037	1.000
Species-environment correlations	.842	.655	.614	.507	
Cumulative percentage variance					
of species data	17.6	29.4	33.9	37.5	
of species-environment relation	43.7	73.1	84.2	93.2	

Figure 10. Results of redundancy analysis: ordination diagram of species and environmental parameters according to axes 1 (43.7%) and 2 (29.4%). The abbreviations of taxa names are from table 3.

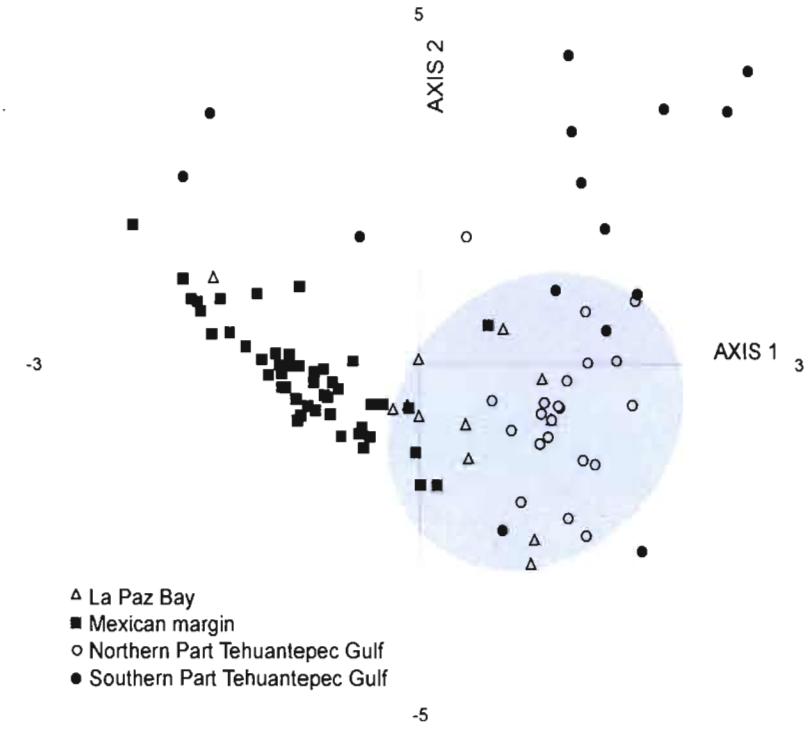

Figure 11. Results from redundancy analysis: ordination diagram of sample scores according to axes 1 and 2, which represent respectively 43.7% and 29.4% of the variance. The blue zone illustrates the similarities between assemblages from sites located in upwelling areas.

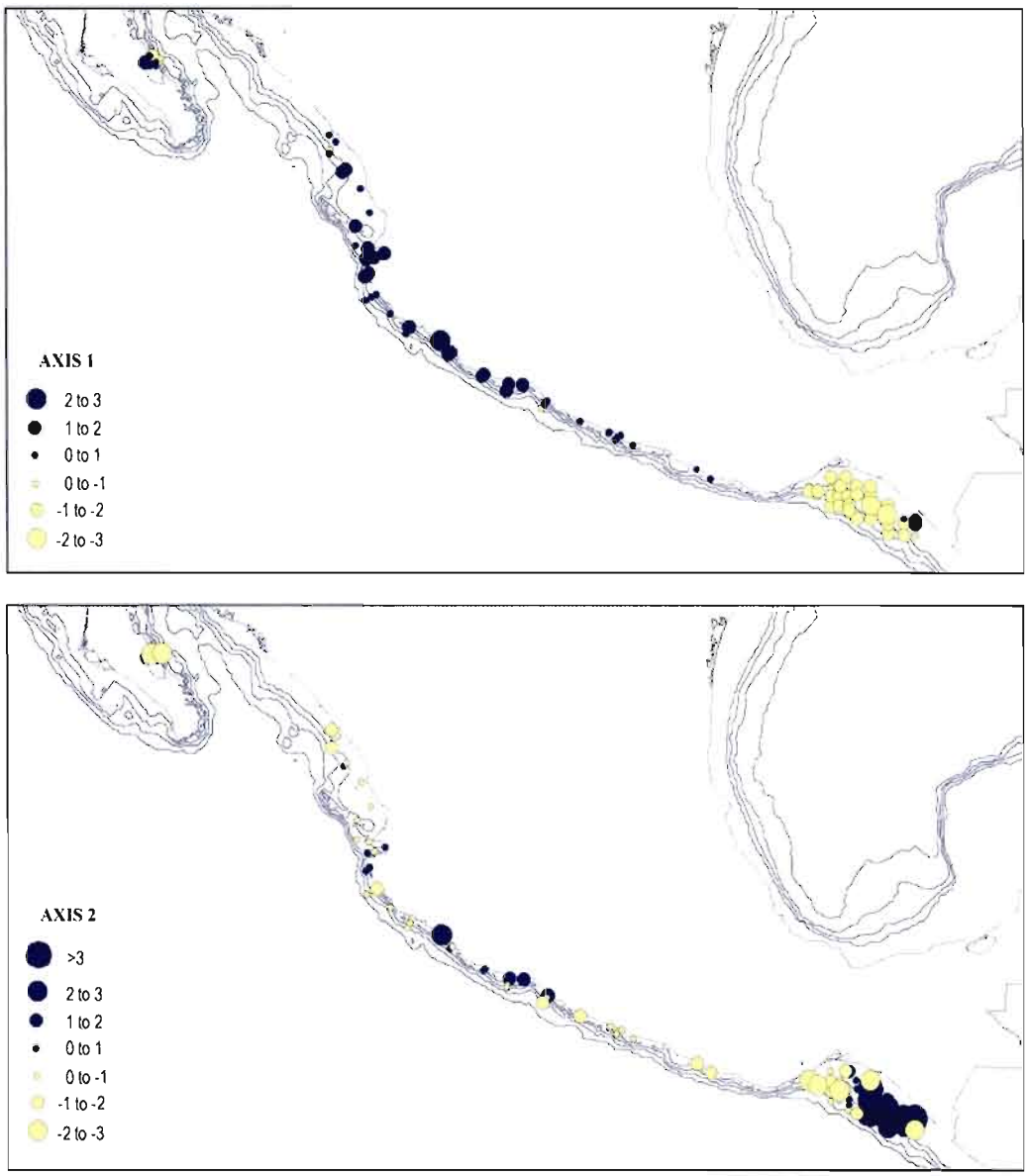

Figure 12. Map showing the sample scores relative to axes 1 and 2 of redundancy analysis. Isobath contours correspond to 200, 500, 1000 and 2000 m.

5. DISCUSSION

5.1 Sources of organic matter

Based on the principle that marine algae are enriched in nitrogen compared to vascular plants, organic carbon to total nitrogen weight ratios (C:N) provide information about the sources of the organic matter deposited in the sediments (Meyer, 1997). While C:N ratios greater than 20 indicate the presence of terrestrial organic matter, marine phytoplankton shows C:N ratios ranging typically between 4 and 10 (Meyer, 1994). In this study, most samples have relatively low C:N ratios (~6 to 10) suggesting dominant fluxes from algae. Samples with higher ratios (~12 to 15.44) reflect fluxes with more land-plant derived organic material.

The carbon isotopic signature ($\delta^{13}C_{org}$) is also used to distinguish types of plants involved in the composition of organic matter, depending on their respective carbon uptake patterns. C_4 land plants (Hatch-Slack pathway; tropical grasses, sedges) have high $\delta^{13}C$ with typical values reaching -14‰, whereas C_3 land plants (Calvin cycle; trees and shrubs) show values around -27‰ (O'Leary, 1988). Marine algae have common average values from -20‰ to -22‰ (Meyers, 1994). In our study area, $\delta^{13}C_{org}$ varies from 21.35‰ to -25.91‰. While values ranging between -21 and -22‰ suggest dominant marine organic matter, more negative $\delta^{13}C$ may be interpreted as marine material mixed with a greater proportion of land–derived organic matter dominated by C_3 plants.

Elevated percentages of organic carbon together with high dinocyst concentrations suggest high productivity throughout the study area. Combined C:N ratios and $\delta^{13}C_{org}$ (Figure 3D) such as dinocyst to pollen grain ratios permit assessment on the sources of organic matter in sediments. They both indicate dominant marine organic carbon over C_3 land-derived material for most samples. The only exception is station 59 where high C:N and dinocyst to pollen grain ratios (22.74 and 0.07) reflect a dominant supply from terrestrial origin. This may be explained by the proximity of the sampling site to the Rio Verde mouth.

5.2 Distribution of dinocyst assemblages in relationship with ocean conditions

The multivariate analyses performed on dinocyst assemblages and environmental parameters demonstrate the determinant role of the distance to the coast and productivity at least at regional scale. Since winter salinity values do not show important variations over the study area, this parameter does not influence significantly the dinocyst distribution.

The nearshore-offshore gradient in the distribution of dinocysts may be related to several parameters which depend upon the distance to the shore. These parameters include turbulence, nutrient availability and water mass stratification. Among these parameters, turbulence is quite important because it limits the dinoflagellate reproduction and the dinocyst growth rates (Gibson and Thomas, 1995; Gibson, 2000). It also leads to heterogeneous mixing and dissipation of both nutrients and dinocysts in the water column and sediment. Based on their respective swimming abilities, it has been demonstrated that dinoflagellates are favoured by well-stratified water oppositely to diatoms, which cannot swim and prefer turbulent waters entraining them up to the surface layer (Gibson and Thomas, 1995). Therefore, blooming of dinoflagellates preferentially occurs under non-turbulent water regimes where they are more competitive with diatoms to use available nutrients (Gibson, 2000).

Productivity is closely related to upwelling. Both La Paz Bay and Tehuantepec Gulf upwelling regions are characterized by the dominance of heterotrophic taxa. This is consistent with previous observations from various upwelling areas (e.g. Lewis et al., 1990; Zonneveld et al., 2001; Dale et al., 2002; Hamel et al., 2002; Radi and de Vernal, 2004). In the present study, dominant taxa are *Brigantedinium* spp., *Echinidinium* spp., *Polykrikos kofoidii* and *Selenopemphix quanta*. Such assemblages are typical of low latitude upwelling regions. Dinocyst assemblages from the Northern part of Tehuantepec Gulf differ from those of La Paz Bay by abundant *Polysphaeridium zoharyi*. Analyses of a core from the northern part of Tehuantepec Gulf demonstrated that the local characteristics of the assemblages did not change significantly during the last centuries with dominant *Brigantedinium* spp. and *Polysphaeridium zoharyi* (c.f. Vasquez-Bedoya et al., 2008).

Taxonomic composition of assemblages from areas of lower productivity level includes higher proportions of phototrophic species, notably *Bitectatodinium spongium* and *Spiniferites* species. *Spiniferites delicatus* seems to be more or less restricted to low productivity or nutrient-depleted areas and it prevails in the Southern part of Tehuantepec Gulf. Since the distribution of phototrophic species depends on light penetration, nutrient availability and competition with other organisms (Taylor and Pollingher, 1987; Gaines and Elbraechter, 1987) their higher proportions in region of lower primary production can be explained by less competition with diatoms (e.g. Radi and de Vernal, 2008).

Statistical analyses performed do not clearly allow the determination of the parameters favourable to red tides. The spatial extent of potentially toxic species is shown in figures 8A and 8B. *P. zoharyi* seems to be eutrophic as its higher abundance is recorded in regions of great productivity and/or high nutrient-level. Concentrations are markedly elevated in the upwelling region of Tehuantepec gulf. Several studies have reported abundant *L. machaerophorum* to occur under eutrophic conditions and have suggested that blooms are driven by nutrient supplies from anthropogenic sources (e.g. Dale et al., 1999; Lewis and Hallett, 1997; Targarona et al., 1999). Herein, this species occurs throughout the study area, but shows higher concentrations near urbanized areas where extensive industrial activities occur, such as Puerto Vallarta, Acapulco and Salina Cruz. However, the continental runoff of nutrients and pollutants due to the industrial development are attenuated by the permanent water mixing due to upwelling making their impact hard to characterize in the area.

6. CONCLUSIONS

The palynological investigation of the western Mexican coast allowed the recognition of distinct assemblages in addition to the relationship between assemblages and the underlying environmental conditions. The distance from the coast and the productivity level are the two parameters that best explain the dinocyst distribution. Cyst associations in upwelling areas are dominated by heterotrophic taxa belonging to Peridiniales and Gymnodiniales with *Brigantedinium* spp., *Echinidinium* spp., *Polykrikos kofoidii* and *Selenopemphix quanta*. The distance to the coast determines turbulence and stratification that both play a role on dinoflagellate populations and the high productivity fosters development of heterotrophic dinoflagellate taxa feeding on diatoms.

The interaction between dinocyst assemblages and environmental conditions is complex and the list of parameters included in statistical analyses is too limited to precisely resolve the conditions favourable to toxic blooms. Water turbulence, lateral transport related to current and wind strength, as well as the nutrient and pollutant supplies are potentially determining. Investigations including these variables would be useful to further document the dinoflagellate to environment relationship. Although we cannot identify the causes of red tides in the study area, we can assess from the dinocyst distribution in sediment that the entire coast of Mexico from 14.81°N to 24.75°N is susceptible to toxic blooms.

CONCLUSION GÉNÉRALE

L'analyse palynologique de la marge Ouest mexicaine a permis de distinguer différents assemblages de dinokystes et d'établir la relation existant entre ces assemblages et les conditions environnementales documentées. La distance par rapport à la côte et la productivité sont les deux paramètres qui se sont révélés être les plus déterminants pour la distribution des dinokystes. La distance par rapport à la côte exerce elle-même un grand contrôle sur le niveau de turbulence et la stratification des eaux. Par ailleurs, la forte productivité favorise la présence d'espèces hétérotrophes pour lesquelles les diatomés sont à la base de la nutrition. Les zones d'upwelling sont dominées par des espèces hétérotrophes de type Péridiniales et Gymnodiniales avec *Brigantedinium* spp., *Echinidinium* spp., *Polykrikos kofoidii* et *Selenopemphix quanta*.

Les interactions entre les assemblages de dinoflagellés et les conditions environnementales sont très complexes et le nombre limité de paramètres environnementaux inclus dans les analyses statistiques ne permet pas d'identifier précisément les conditions favorables à la formation des marées rouges. La turbulence des eaux, le transport latéral lié aux courants et aux vents, ainsi que l'apport en nutriments et en polluants sont également des paramètres potentiellement déterminants. Une étude concernant ces variables pourrait être très utile pour améliorer notre compréhension de la relation entre les dinoflagellés et leur environnement. Bien que nous n'ayons pu identifier les causes exactes du phénomène de marées rouges dans la zone d'étude, la distribution des dinokystes dans les sédiments nous permet de constater que l'ensemble de la côte Ouest du Mexique de 14.81°N jusqu'à 24.75°N est susceptible d'être affectée par des blooms toxiques.

APPENDICE A

TABLEAU DE DÉNOMBREMENT DES PALYNOMORPHES

Tableau 1. Dénombrement des palynomorphes terrestres (grains de pollens) et marins (dinokystes et réseaux organiques de foraminifères) de la marge Ouest mexicaine.

Stations	*Bitectatodinium spongium*	*Lingulodinium machaerophorum*	*Nematosphaeropsis labyrinthus*	*Operculodinium centrocarpum*	*Polysphaeridium zoharyi*	*Spiniferites delicatus*	*Spiniferites elongatus*	*Spiniferites ramosus*	*Spiniferites mirabilis*	*Spiniferites* spp.	Cyst of *Pentapharsodinium dalei*	*Brigantedinium* spp.	*Lejeunecysta* spp.	*Selenopemphix nephroides*	*Selenopemphix quanta*	Cyst of *Protoperidinium nudum*	*Votadinium* spp.	Cyst of *Protoperidinium americanum*	*Quinquecuspis concreta*	Cyst of *Polykrikos schartzii*	Cyst of *Polykrikos kofoidii*	Cyst of cf. *Polykrikos kofoidii*	*Echinidinium aculeatum*	*Echinidinium granulatum*	*Echinidinium delicatum*	*Echinidinium transparantum*	*Echinidinium* spp.	Cyst A	*Tuberculodinium vacampoea*	**Total dinokystes**	**Total réseaux organiques**	**Total grains de pollens**
13	33	2	5	7	4	0	0	3	0	4	11	102	0	8	3	3	0	0	0	2	21	6	12	59	1	21	3	1	0	314	239	267
14	46	3	6	3	1	3	0	4	0	5	6	77	0	4	6	2	0	1	0	0	12	15	25	59	5	18	7	0	0	315	259	211
15	31	18	3	8	113	29	0	16	3	11	0	8	0	1	3	2	0	0	0	0	5	11	4	27	0	13	0	1	2	310	108	315
16	28	3	0	0	0	0	0	4	2	4	0	98	0	11	5	5	0	0	3	0	1	3	25	45	5	39	2	2	0	288	435	477
17	24	3	3	0	0	0	0	0	0	0	7	28	0	0	3	5	0	3	2	2	1	0	3	20	0	15	2	0	0	122	446	167
18	60	11	5	1	1	3	0	4	0	0	2	52	0	7	3	3	0	2	6	0	7	9	15	45	6	16	2	0	0	269	581	394
19	25	26	12	8	3	0	2	16	0	5	14	35	1	1	2	2	0	3	0	10	0	18	10	59	4	17	3	0	0	302	250	375
20	44	21	7	1	3	2	0	17	0	6	12	53	0	0	4	14	0	2	0	3	6	15	12	42	5	19	6	2	2	300	249	341
21	33	7	0	2	0	0	0	3	0	4	10	53	1	2	13	12	0	1	0	1	6	6	33	63	3	40	4	0	0	304	83	202
22	13	2	0	1	0	0	0	0	0	1	2	71	0	1	11	2	1	2	2	0	3	2	43	65	3	71	5	0	0	316	193	290
23	36	27	1	0	0	0	0	1	0	0	0	37	0	0	6	4	0	3	1	0	6	1	4	10	3	14	3	0	0	164	144	58
24	64	18	2	2	1	0	0	0	0	1	3	43	0	1	8	2	0	4	0	1	9	2	31	66	6	25	1	1	0	309	52	167
25	32	7	1	4	1	1	0	0	0	0	5	40	1	2	7	3	0	2	0	1	5	7	46	76	7	36	1	1	0	306	39	294
26	111	41	0	0	1	1	0	3	1	1	1	46	0	0	3	1	0	4	1	0	1	0	21	30	3	19	3	0	0	308	37	554
27	95	0	0	3	0	2	0	9	0	3	0	20	0	0	23	1	0	1	3	0	28	20	19	54	9	29	0	0	0	334	22	69
28	41	1	0	3	0	6	0	2	0	2	0	38	0	0	17	20	0	3	0	0	9	4	51	59	12	40	1	0	0	318	18	106
29	22	0	0	4	2	5	0	1	0	1	1	75	1	0	11	22	0	1	0	0	2	9	30	63	11	35	8	0	0	313	46	115
30	28	0	1	1	0	0	0	0	0	0	2	75	0	1	13	11	0	0	2	0	3	1	49	76	10	36	4	0	0	321	106	224

Stations	*Biectatodinium spongium*	*Lingulodinium machaerophorum*	*Nematosphaeropsis labyrinthus*	*Operculodinium centrocarpum*	*Polysphaeridium zoharyi*	*Spiniferites delicatus*	*Spiniferites elongatus*	*Spiniferites ramosus*	*Spiniferites mirabilis*	*Spiniferites* spp.	Cyst of *Pentapharsodinium dalei*	*Brigantedinium* spp.	*Lejeunecysta* spp.	*Selenopemphix nephroides*	*Selenopemphix quanta*	Cyst of *Protoperidinium nudum*	*Votadinium* spp.	Cyst of *Protoperidinium americanum*	*Quinquecuspis concreta*	Cyst of *Polykrikos schartzii*	Cyst of *Polykrikos kofoidii*	Cyst of cf. *Polykrikos kofoidii*	*Echinidinium aculeatum*	*Echinidinium granulatum*	*Echinidinium delicatum*	*Echinidinium transparantum*	*Echinidinium* spp.	Cyst A	*Tuberculodinium vacampoea*	**Total dinokystes**	**Total réseaux organiques**	**Total grains de pollens**
31	18	4	0	0	0	4	0	0	0	0	0	69	0	1	4	1	0	8	0	0	12	3	9	29	12	11	5	0	0	198	45	193
32	43	4	0	4	0	5	1	4	0	2	0	70	0	0	8	9	0	7	0	0	2	7	24	34	13	32	5	1	0	297	34	276
33	7	2	0	0	0	1	0	4	2	1	1	15	0	0	4	0	0	8	1	0	1	0	0	7	5	5	0	0	0	67	16	182
34	63	2	0	1	1	0	0	13	0	2	3	33	0	0	14	5	0	0	0	0	9	2	35	33	7	65	5	0	0	303	10	251
35	50	1	2	1	1	0	0	13	0	0	0	86	0	1	10	6	0	8	2	1	10	5	14	49	7	34	0	0	0	311	50	395
36	21	1	0	1	26	0	1	9	0	6	6	46	0	1	18	8	0	10	0	0	5	2	29	77	21	20	6	0	0	315	36	207
37	33	1	0	0	1	0	0	3	0	0	0	2	0	0	3	0	0	1	1	0	1	6	5	0	3	2	1	0	0	64	72	153
38	103	2	3	1	0	1	0	10	1	2	0	44	0	0	4	7	0	1	0	0	7	6	24	22	16	30	1	0	0	301	51	225
39	28	2	0	0	1	0	1	2	1	6	2	31	0	0	9	0	0	0	0	0	2	1	20	21	8	19	2	0	0	161	112	380
40	87	1	0	1	0	0	1	4	6	2	0	34	0	0	12	10	0	3	0	0	4	3	29	50	5	36	0	0	0	302	120	292
41	41	0	0	0	1	3	0	12	3	7	0	42	0	2	12	5	0	8	0	0	8	2	8	32	1	27	1	0	0	228	262	414
42	83	1	2	1	0	4	0	3	0	1	1	57	0	1	6	4	0	6	0	0	0	0	28	48	3	48	5	0	2	307	121	684
43	28	1	0	2	0	1	0	7	0	0	4	62	0	2	9	6	0	3	0	0	8	2	55	67	8	26	6	0	2	304	121	468
44	67	2	0	0	0	2	0	3	0	2	0	92	0	0	6	1	0	5	0	0	2	3	27	67	4	34	4	0	0	323	65	579
45	32	1	0	0	0	1	0	1	0	1	2	13	0	1	3	0	0	1	0	1	2	0	3	3	0	13	0	0	0	78	77	515
46	92	1	0	3	3	13	1	8	2	10	1	41	0	2	14	6	0	2	0	0	5	4	26	40	0	26	1	0	0	307	121	294
47	74	15	0	2	6	25	1	11	5	10	2	34	0	1	8	5	0	2	0	0	6	4	26	36	8	23	0	0	0	313	412	252
48	35	6	0	0	10	9	3	3	3	8	2	89	0	0	4	1	1	3	4	0	14	10	19	40	9	13	1	0	0	309	288	596
49	33	4	0	1	12	13	0	5	8	8	5	46	3	2	8	6	0	0	1	2	11	6	32	33	2	23	0	0	0	270	265	299
50	7	2	0	0	5	0	0	0	2	3	1	61	0	0	3	2	0	2	0	0	0	0	17	25	1	9	1	0	0	142	142	148

Stations	51	52	53	54	55	56	57	58	59
Bitectatodinium spongium	6	33	37	27	32	20	7	12	4
Lingulodinium machaerophorum	0	4	2	19	8	0	2	0	1
Nematosphaeropsis labyrinthus	0	0	0	0	0	0	0	1	0
Operculodinium centrocarpum	0	1	1	0	0	0	0	3	0
Polysphaeridium zoharyi	2	0	3	22	5	11	13	0	0
Spiniferites delicatus	2	1	0	1	0	0	1	1	0
Spiniferites elongatus	0	0	0	0	0	0	0	0	1
Spiniferites ramosus	0	10	2	9	0	0	1	0	3
Spiniferites mirabilis	0	1	0	2	2	1	2	0	2
Spiniferites spp.	3	4	0	7	7	3	0	4	0
Cyst of *Pentapharsodinium dalei*	0	0	0	0	0	0	0	1	0
Brigantedinium spp.	71	34	73	55	49	52	19	108	21
Lejeunecysta spp.	0	0	0	1	1	0	0	0	0
Selenopemphix nephroides	2	0	1	3	7	2	1	7	1
Selenopemphix quanta	7	5	5	7	3	6	9	6	5
Cyst of *Protoperidinium nudum*	5	0	1	1	9	1	1	4	0
Votadinium spp.	0	0	0	0	0	0	0	0	0
Cyst of *Protoperidinium americanum*	1	1	1	1	2	1	5	7	0
Quinquecupsis concreta	0	0	11	5	7	3	4	2	3
Cyst of *Polykrikos schartzii*	0	0	0	0	0	1	0	0	0
Cyst of *Polykrikos kofoidii*	5	16	9	14	13	12	2	3	4
Cyst of cf. *Polykrikos kofoidii*	4	7	7	22	5	3	4	6	0
Echinidinium aculeatum	12	7	14	16	10	39	7	61	4
Echinidinium granulatum	24	17	32	22	47	118	16	51	3
Echinidinium delicatum	2	1	0	4	0	2	2	60	1
Echinidinium transparantum	6	9	2	14	6	13	3	8	2
Echinidinium spp.	2	2	4	1	1	6	5	20	1
Cyst A	0	0	0	0	0	0	3	0	0
Tuberculodinium vacampoea	0	1	0	0	0	0	0	0	0
Total dinokystes	163	161	209	262	233	301	116	369	60
Total réseaux organiques	196	154	283	199	122	44	55	50	99
Total grains de pollens	272	272	222	264	396	611	557	220	946

APPENDICE B

PLANCHES PHOTOGRAPHIQUES

PLATE 1

Note. Scale bars correspond to 20 μm. Sample numbers are followed by England Finder coordinates and the laboratory reference numbers of the slides.

1-3. *Bitectatodinium spongium*
1-2. Tehua V Est. 2, N15. 03, n° 2407-02;
3. Tehua V Est. 2, G17.03, n° 2407-02.

4-5. *Polysphaeridium zoharyi*
4-5. Tehua V Est. 3, T34.04, n° 2407-03.

6. *Operculodinium centrocarpum*
6. Tehua V Est. 3, J14.04, n°2407-03.

7-8. *Lingulodinium machaerophorum*
7-8. Tehua V Est. 7, S29.03, n°2407-06 (Processes view).

9. *Tuberculodinium vancampoae*
9. Tehua V Est. 4, N29.03, n°2434-06

10-11-12. Cyst of *Gymnodinium catenatum*
10. Tehua V Est. 39, T18.03, n°2426-02
11-12. Tehua V Est. 39, Q29.01, n°2426-02

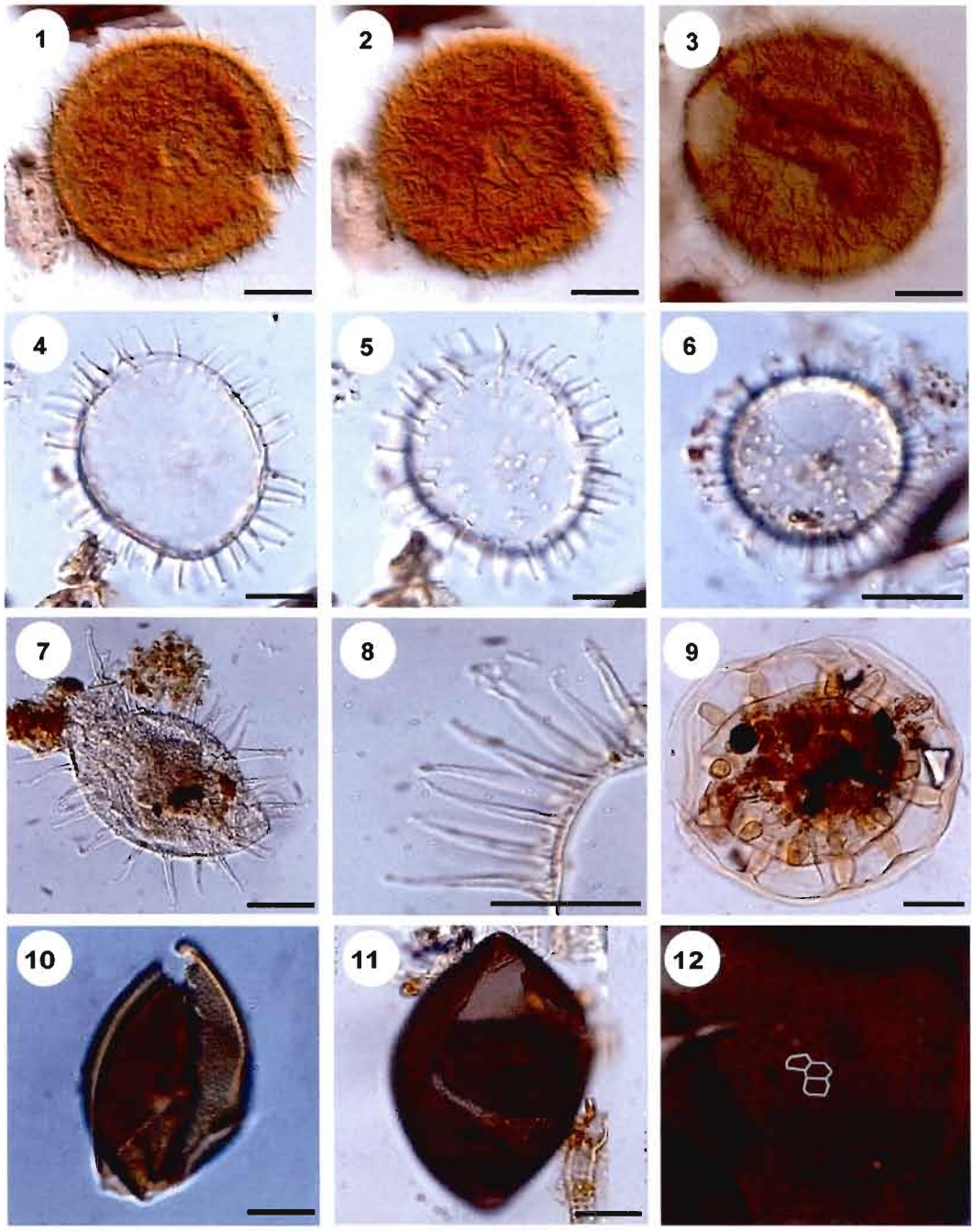

Plate 1. Micrographs of selected dinocyst taxa:
1-3. *Bitectatodinium spongium*; 4-5 *Polysphaeridium zoharyi*; 6. *Operculodinium centrocarpum*; 7-8. *Lingulodinium machaerophorum*; 9. *Turberculodinium vancampoae;* 10-11. Cyst of *Gymnodinium catenatum*; 12. Reticulation on the surface of cyst of *Gymnodinium catenatum.* Scale bars: 20μm

PLATE 2

Note. Scale bars correspond to 20 μm. Sample numbers are followed by England Finder coordinates and laboratory reference numbers of the slides.

1-2. *Spiniferites delicatus*
1-2. Tehua V Est. 3, K25.03, n°2407-03.

3-4. *Spiniferites ramosus*
3-4. Tehua V Est. 3, K23.03, n°2407-03.

5. *Nematosphaeropsis labyrinthus*
5. Tehua V Est. 3, L41.02, n°2407-03.

6. *Echinidinium* sp.1
6. Tehua V Est. 2, D19.02, n°2407-02

7. Cyst type A
7. Paleo IX, Est. 22, F30.03n°1945-01

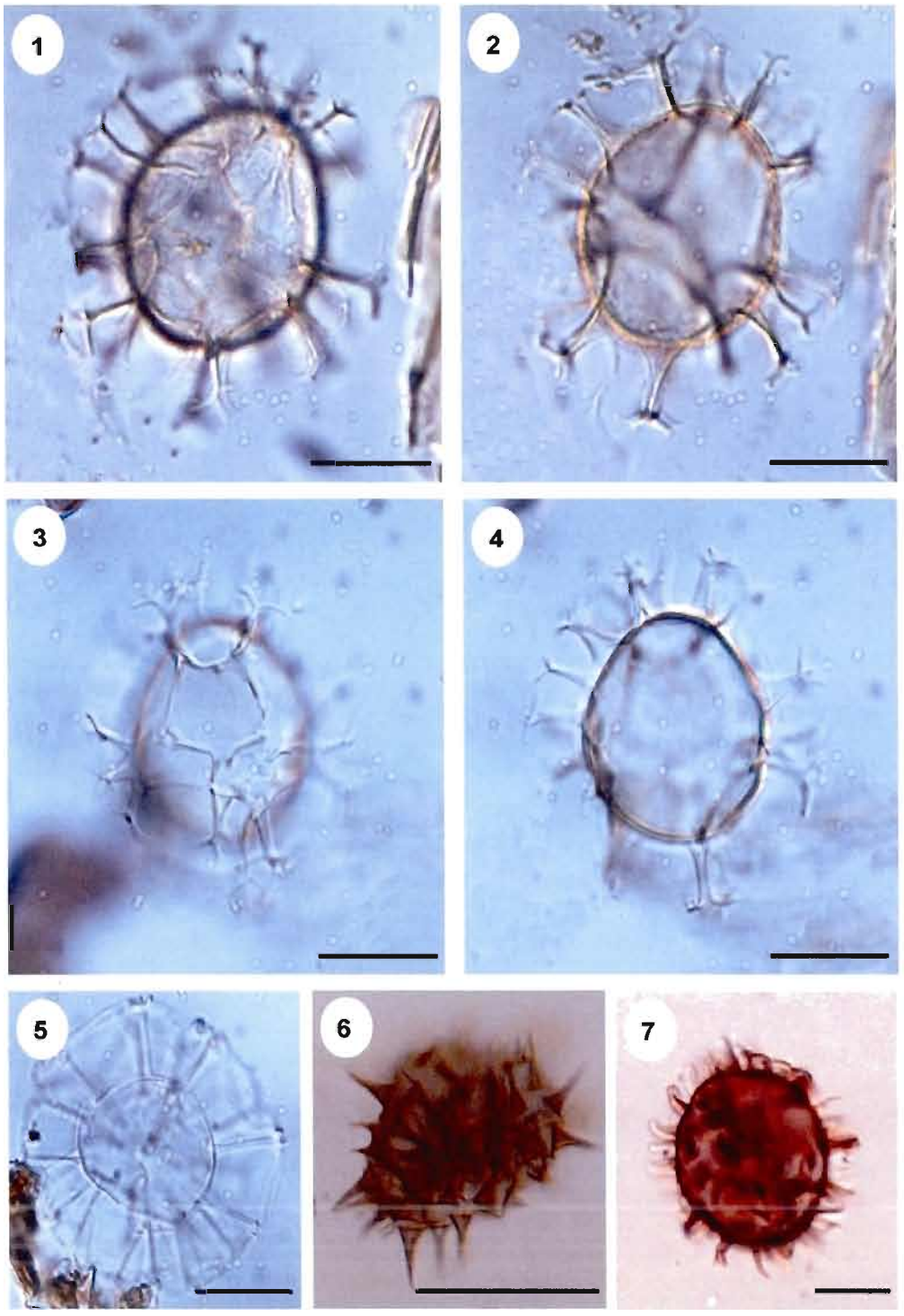

Plate 2. Micrographs of selected dinocyst taxa:
1-2. *Spiniferites delicatus*; 3-4. *Spiniferites ramosus*; 5. *Nematosphaeropsis labyrinthus;* 6. *Echinidinium* sp.1; 7. Cyst A. Scale bars: 20µm

PLATE 3

Note. Scale bars correspond to 20 μm. Sample numbers are followed by England Finder coordinates and laboratory reference numbers of the slides.

1. Cyst of *Polykrikos kofoidii*
1. Tehua V Est. 1, F19.02, n°2407-01

2-3. Cyst of *Polykrikos* cf. *kofoidii*
2. Tehua V Est. 1, N06.06, n°2407-01
3. Tehua V Est. 1, E27.04, n°2407-01

4-5. Cyst of *Polykrikos schwartzii*
4. Tehua V Est. 1, N12.03, n°2434-05
5. Tehua V Est. 1, J42.01, n°2434-05

6. *Selenopemphix nephroides*
6. Tehua V Est. 7, Q28.04, n°2407.06

7. *Selenopemphix quanta*
7. Tehua V Est. 39, B30.03, n°2426-02

8. Cyst of *Protoperidinium nudum*
8. Tehua V Est. 4, W07.02, n°2407-04

9. *Stelladinium spp.*
9. Paleo IX Est. 39, P52.04, n°1945-05

10. *Quinquecupsis concreta*
10. Tehua Est. 36, S19.04, n°2070-03

11. *Votadinium spinosum*
11. Paleo IX Est. 34, J47.02, n°2098-04

12. *Votadinium calvum*
12. Tehua Est. 10, F22.04, n°1946-02

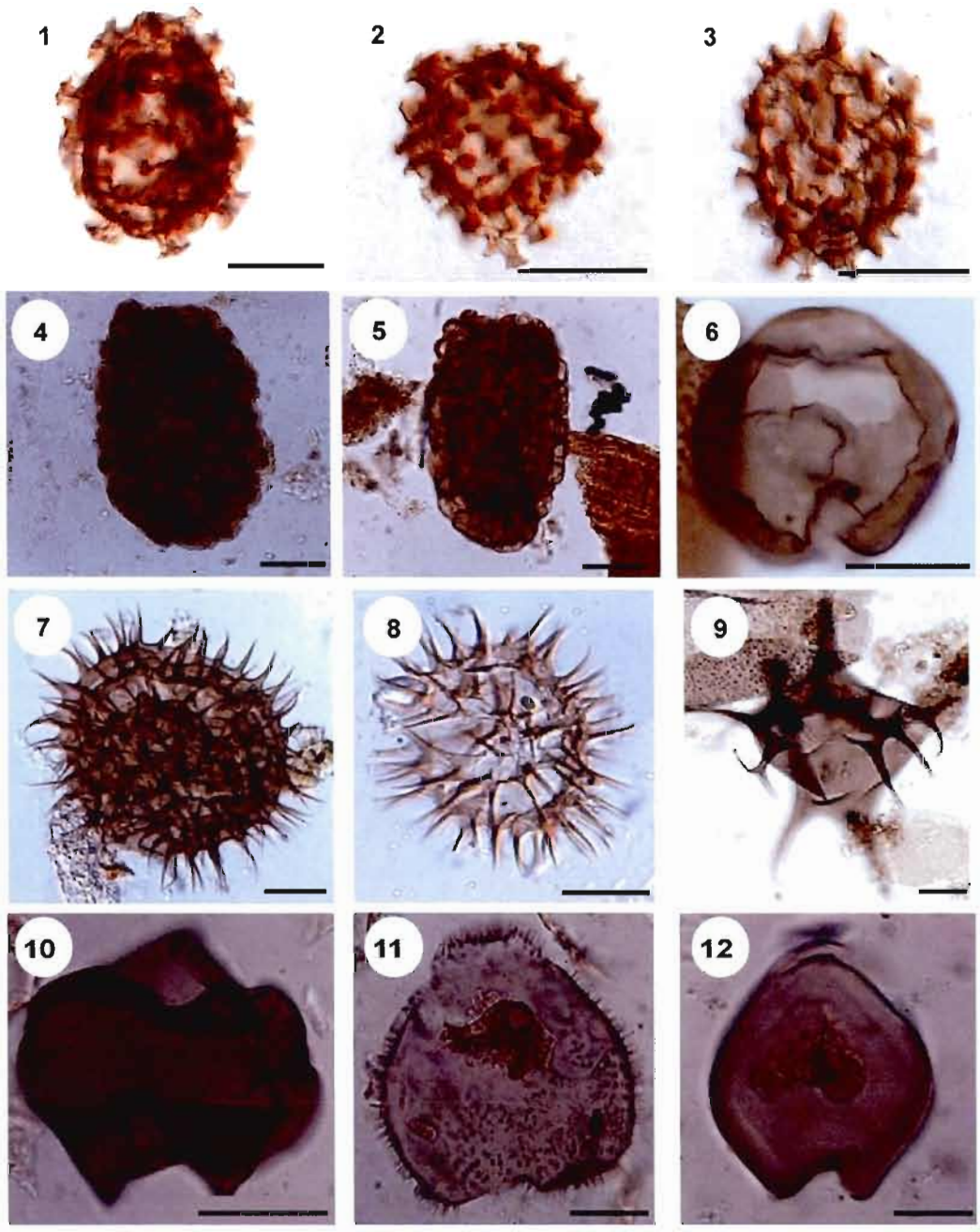

Plate 3. Micrographs of selected dinocyst taxa:
1 *Polykrikos kofoidii*; 2-3. *Polykrikos* cf. *kofoidii*; 4-5 *Polykrikos schwartzii*;
6. *Selenopemphix nephroides*; 7. *Selenopemphix quanta*; 8. Cyst of *Protoperidinium nudum*;
9. *Stelladinium* spp.; 10. *Quinquecupsis concreta*; 11. *Votadinium spinosum*; 12. *Votadinium calvum*. Scale bars: 20μm

PLATE 4

Note. Scale bars correspond to 20 µm. Sample numbers are followed by England Finder coordinates and laboratory reference numbers of the slides.

1. *Echinidinium delicatum*
   1. Tehua V Est. 2, F20.03, n°2407-02

2. *Echinidinium transparantum*
   2. Tehua V Est. 2, B30.04, n°2407-02

3. *Echinidinium aculeatum*
   3. Tehua V Est. 4, J27.04, n°2407-04.

4. *Echinidinium granulatum*
   4. Tehua V Est. 3, L38.02, n°2407.03.

Schemas have been made by Radi Taoufik.

Schemas **Micrographs**

Echinidinium delicatum

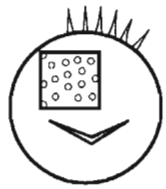

1

Echinidinium transparantum

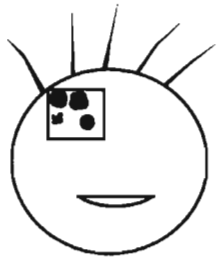

2

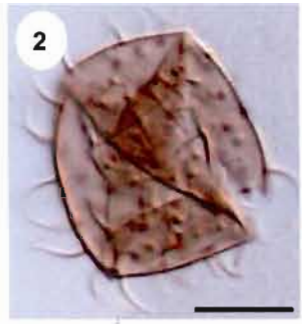

Echinidinium aculeatum

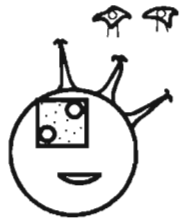

3

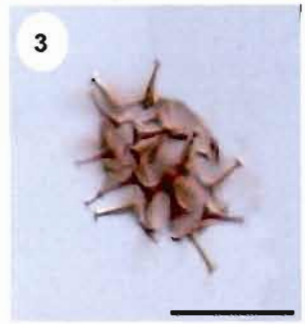

Echinidinium granulatum

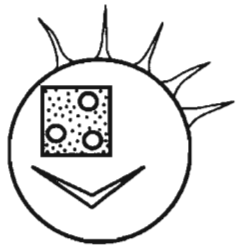

4

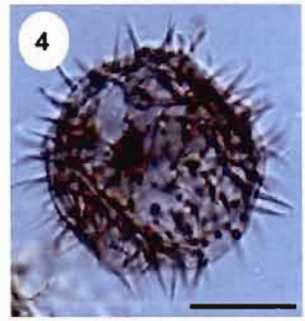

Plate 4. Schemas (Radi) and micrographs of selected dinocyst taxa:
1. *Echininidinum delicatum;* 2. *Echinidinium transparantum*;
3. *Echininidinum aculeatum;* 4. *Echinidinium granulatum.*
Scale bars: 20μm

APPENDICE C

SYSTÉMATIQUE

Class DINOPHYCEAE Pascher 1914

Order GONYAULACALES Taylor, 1980

Family GONYAULACACEAE Lindemann, 1928

Subfamily CRIBROPERIDINIOIDEAE Fensome et al., 1993a

Genus *Lingulodinium* Wall 1967 emend. Dodge 1989

Lingulodinium machaerophorum

(Deflandre & Cookson, 1955) Wall, 1967

(Plate 1, figs. 7-8)

Dimensions. Central body diameter 38-50 μm; Process length up to 21 μm (Reid, 1974).

Distinguishing characters. Specimens from the North and Tropical Eastern Pacific show typical morphological features and are characterized by a spherical central body with finely but distinctly granulate wall surface. Processes are non-tabular, hollow and closed distally. They arise from a circular base, taper distally and tend towards flattening. They usually terminate as a pointed or blunt tip. Processes usually have a smooth surface but small spinules may occur over the distal part. The archeopyle is formed by the loss of one or more precingular plates.

Biological affinity. *Lingulodinium polyedrum*

Genus *Operculodinium* Wall 1967 emend. Matsuoka et al. 1997

Operculodinium centrocarpum

sensu Wall & Dale 1966

(Plate 1, fig. 6)

Dimensions. Central body diameter: 33-48 μm; Process length: 7-14 μm.

Distinguishing characters. Spherical central body bearing numerous slender processes whose distribution does not clearly reflect tabulation. The surface has scattered granules or columellae, often fine and faintly visible with interconnecting fibrils sometimes discernible. Processes are hollow, circular in cross-section and distally open. They have a smooth surface, may broaden slightly at their base and are expanded at the tips. Archeopyle has rounded angles and is formed by loss of a single precingular plate (3''). Some rare specimens of *O. centrocarpum* morphotype short processes have been recorded in the North Eastern Pacific.

Biological affinity. *Protoceratium reticulatum*

Subfamily GONYAULACOIDEAE (Autonym)

Genus *Bitectatodinium* Wilson, 1973

Bitectatodinium spongium

(Zonneveld, 1997) emend. Zonneveld and Jurkschat, 1999

(Plate 1, figs. 1-3)

Dimensions. Central Body diameter (excluding luxuria): 40-75 μm; Maximum fibril length: 9-12 μm; Twenty-four specimens were measured (this study).

Distinguishing characters. Specimens from the Tropical Eastern Pacific are similar to those described in the Arabian Sea by Zonneveld (1997): a proximate cyst with a spherical to ovoidal body, a thin endophragm and a periphragm characterized by numerous spongy, granulo-fibrous, distally open spines with minutely expanded tips or acuminate solid fibres. The precingular archeopyle is expressed by the loss of 2" and 3".

Biological affinity. Unknown

Genus *Nematosphaeropsis* Deflandre & Cookson 1955 emend. Wrenn 1988

Nematosphaeropsis labyrinthus

(Ostenfeld, 1903) Reid, 1974

(Plate 2, fig. 5)

Dimensions. Central body length: 27-42 μm; Maximum process height: 11-23 μm; (Reid, 1974; Rochon et al., 1999).

Distinguishing characters. Trabeculate cyst with an ovoid central body. Surface of central body and processes are smooth. Processes are exclusively gonal in distribution and have hollow, slender shafts with distal trifurcations. Distal branches are linked by parallel pairs of ribbon-like trabeculae, about 1.0 to 1.5μm wide, which reflected plate sutures. Archeopyle precingular formed by loss 3'' plate.

Biological affinity. Unknown, but probably belonging to the *Gonyaulax spinifera* complex.

Genus *Polysphaeridium* Davey & Williams 1966

Polysphaeridium zoharyi

(Rossignol, 1962) Bujak et al., 1980

(Plate 1, figs. 4-5)

Dimensions. Cyst body diameter: 42 to 75 μm; Length of processes: 6 to 15 μm; Twenty-one specimens measured (this study).

Distinguishing characters. Chorate cyst with a spherical central body, smooth to microreticulate-microgranulate wall surface. Processes are numerous (~ 60), hollow, opened distally with a variable length and a weakly striated base. Processes can be fused at their bases or distally bifurcate. Epicystal archeopyle.

Biological affinity. *Pyrodinium bahamense*

Genus *Spiniferites* Mantell 1850 emend. Sarjeant 1970

Spiniferites delicatus

(Reid, 1974)

(Plate 2, figs. 1-2)

Dimensions. Central body length: 40-60 μm (Reid, 1974).

Distinguishing characters. Spiniferate cyst having ovoidal central body with both inner and outer wall layers microgranular. A low apical boss was distinguishable on most specimens. Processes are membranous, mostly gonal with petaloid process tips. Sutural crests are high and membranous. Both processes and crests have faintly granular surfaces. Archeopyle formed by loss of plate 3''.

Biological affinity. Unknown, but probably belonging to *Gonyaulax* sp.

Spiniferites elongatus

(Reid, 1974)

Dimensions. Endoblast length: 40-59μm (Reid, 1974).

Distinguishing characters. Spiniferate cyst having a conspicuously elongate central body and a smooth to finely microgranulate surface. Sutural crests are membranous and hollow, and vary in height, being low around the cingulum and mostly high on the hypocyst and towards the apex. However, some specimens exhibit low sutural crests and processes at the

apex and antapex. Processes are mostly gonal and trifurcate and are often extensions of these crests. Archeopyle formed by loss of plate 3''.

Biological affinity. *Gonyaulax spinifera*

Spiniferites membranaceus

(Rossignol, 1964) Sarjeant, 1970

Dimensions. Endoblast length: 34-44 μm (Reid, 1974).

Distinguishing characters. Rare specimens have been observed in the North and Tropical Eastern Pacific. *Spiniferites membranaceus* is a spiniferate cyst having ovoidal central body with microgranular to microreticulate surface and small apical boss. Processes are gonal and occasionally intergonal. They are distally furcate with recurved bifurcate tips. Sutural crests are mostly low but are high at the antapex where they form a conspicuous membrane between antapical processes. Archeopyle formed by loss of plate 3''.

Biological affinity. *Gonyaulax spinifera*

Spiniferites mirabilis

(Rossignol, 1964) Sarjeant, 1970

Dimensions. Endoblast length: 44-58 μm (Reid, 1974)

Distinguishing characters. Spiniferate cysts having a broadly ovoidal to spheroidal central body. Surface of outer wall is microgranulate. Processes are both gonal and intergonal and are distally furcate with recurved bifurcate tips. Sutural crests are low or absent except a the antapex where they form a broad and conspicuous flange between antapical processes. Archeopyle formed by loss of plate 3''.

Biological affinity. *Gonyaulax spinifera*

Spiniferites ramosus

(Ehrenberg, 1837) Mantell 1854 sensu lato

(Plate 2, figs. 3-4)

Dimensions. Endoblast length: 30-46 μm (Rochon et al., 1999).

Distinguishing characters. Spiniferate cyst with ovoidal to spherical central body and no apical boss. Surface of inner and outer wall smooth. Processes are exclusively gonal. They are long, hollow and have long distal furcations with bifurcate tips. Sutural crests are low but rise towards the gonal processes to which they connect. Archeopyle formed by loss of plate 3''.

Biological affinity. *Gonyaulax spinifera* complex

Class DINOPHYCEAE Pascher 1914

Subclass PERIDINIPHYCIDAE Fensome et al. 1993a

Order GYMNODINIALES Lemmermann

Family GYMNODINIACEAE (Bergh) Lankester

Genus *Gymnodinium* Stein

Gymnodinium catenatum

(Graham, 1943)

(Plate 1, figs. 10-11-12)

Dimensions. Central body length: 38-60 μm (mean 49 μm); Wall thickness: 0.6-1 μm; Polygonal areas, longest dimension: 3 μm.

Distinguishing characters. Spherical cyst, unless excystment has occurred. Most specimens observed in this study seem to be excysted and resemble *Taxodium*-type pollen in that the cyst splits and gapes open to a varying degree subequatorially. As observed, the halves may or may not be attached along a narrow isthmus of cyst wall. Autophragm; internally smooth but covered externally by a dense microreticulum (fig. 12) of low (<0.2 μm) rounded ridges.

Biological affinity. *Gymnodinium catenatum*

Family POLYKRIKACEAE Kofoid & Swezy 1921

Genus *Polykrikos* Bütschli 1873

Cyst of *Polykrikos kofoidii*

(Chatton, 1914)

(Plate 3, fig. 1)

Dimensions. Central body length: 40-82 μm; Maximum process length: 10-27 μm; Fifteen specimens were measured (this study).

Observations. Dark brown elongated cyst. Cysts of *Polykrikos kofoidii* were described as having separate shirt and large cylindrical processes. Note that specimens bearing discontinuous, distally-flared ridges were referred to as *Polykrikos* sp. cf. *P. kofoidii* (e.g. Matsuoka, 1985).

Biological affinity. Recent phylogenetic and rDNA analyses by Matsuoka et al. (2009) have demonstrated that cyst of *Polykrikos kofoidii* as identified herein correspond to the motile-stage of *Polykrikos schwartzii* (see Matsuoka et al., 2009).

Cyst of *Polykrikos* cf. *kofoidii*

(Chatton, 1914)

(Plate 3, figs. 2-3)

Dimensions. Central body length: 25-65 μm; Maximum process length: 4.5-11 μm; Twelve specimens were measured (this study).

Observations. Cysts within the smaller part of the size range for *P. kofoidii*, processes relatively short, abundant and more spongy than fibrous. Central body more oval than *P. kofoidii*. The cysts of *P.* cf. *kofoidii* are found off California and along the western Mexican coast.

Cyst of *Polykrikos schwartzii*

(Bütschli, 1873)

(Plate 3, figs. 4-5)

Dimensions. Central body length: 54-80 μm; Maximum reticulation height: 5-8 μm; Seven specimens were measured (this study).

Distinguishing characters. A large elongate cyst with medium to dark brown wall. Cysts of *Polykrikos schwartzii* are recognizable and consistently different from those of *Polykrikos kofoidii*. Cysts wall of *Polykrikos schwartzii* bears ornamentation that comprises a more-or-less complete reticulum, whereas the cyst wall of *Polykrikos kofoidii* has ornamentation that varies from discrete cylindrical processes to ridges forming only a partial reticulum (see under *Polykrikos kofoidii*).

Biological affinity. Recent phylogenetic and rDNA analyses by Matsuoka et al. (2009) have demonstrated that cyst of *Polykrikos schwartzii* as identified herein correspond to the motile-stage of *Polykrikos kofoidii* (see Matsuoka et al., 2009).

Order PERIDINIALES Haeckel 1894
Family GONIODOMACEAE Lindemann 1928

Genus *Tuberculodinium* Wall 1967

Tuberculodinium vancampoae

(Rossignol, 1962)
(Plate 1, fig. 9)

Dimensions. Cyst diameter: 84.3 μm; Length of processes: 13 μm.

Distinguishing characters. Discoidal cyst with two wall-layers, the outer wall being supported above the inner wall by numerous short, tuberculate projections. Dorsal surface with a large compound archeopyle, which probably corresponds to a combination of precingular and intercalary plates.

Biological affinity. *Pyrophacus steinii*

Family PERIDINIACEAE Ehrenberg 1831
Subfamily CALCIODINELLOIDEAE Fensome et al. 1993a

Genus *Pentapharodinium* Indelicato & Loeblich III 1986 emend. Montresor et al. 1993

Cyst of *Pentapharsodinium dalei*

(Indelicato & Loeblich III, 1986)

Dimensions. Central body diameter: 19-36 μm; Process length: 1-8 μm (Dale, 1977)

Distinguishing characters. Small colorless cyst with spherical central body and solid processes that may be branched or unbranched, both types usually being present on a single

specimen. Processes may branch at any point along their length. They are often minutely branched at their tips and may broaden proximally. Broader and more slender processes may occur on a single cyst. The central body wall is thin (less than 0.5 μm) and has a smooth surface. There is no indication of tabulation.

Biological affinity. *Peridinium faeroense*

Family PROTOPERIDINIACEAE Balech 1988

Genus *Brigantedinium Reid* 1977 ex Lentin & Williams 1993

Brigantedinium simplex

(Wall, 1965) ex. Lentin & Williams 1993

Dimensions. Diameter: 29-54 μm (Wall, 1965; Reid, 1977).

Distinguishing characters. Spherical cyst having a smooth surface. Wall is brown pigmented and usually single layered. Two depressions may occur in the ventral region representing flagellar scars. The archeopyle is intercalary (2a) and asymmetrically hexagonal with height and breadth being approximately equal. There is usually no accessory archeopyle suture. Observation of the archeopyle was rarely possible on specimens from the Eastern Tropical Pacific. Therefore, *Brigantedinium simplex* has been identified as *Brigantedinium* spp. in this study.

Biological affinity. *Protoperidinium conicoides*

Genus *Protoperidinium Bergh 1881*

Cyst of *Protoperidinium americanum*

(Gran & Braarud, 1935) Balech 1974

Dimensions. Central body diameter: 34-52 μm (Lewis and Dodge, 1987; Rochon et al., 1999).

Distinguishing characters. Cyst with a brown-pigmented spherical central body and a transparent, loosely-appressed outer membrane. The central body wall consists of a thin, solid inner layer and a thicker, closely-appressed, granular outer layer. The overlying outer membrane is thin, smooth and folded. The archeopyle on the central body appears to be formed by separate release of the second, third and foutth apical plates. Accessory sutures may be present. The archeopyle on the outer membrane is difficult to distinguish due to tearing and folding. There is no other indication of tabulation.

Biological affinity: *Protoperidinum americanum*

Cyst of *Protoperidinium nudum*

(Meunier, 1919) Balech 1974?

(Plate 3, fig. 8)

Dimensions. Central body diameter: 35-40 μm; Four specimens were measured (this study).

Distinguishing characters. Small, spiny, brown-pigmented cyst similar to cyst of *P. nudum*? in Wall and Dale (1968, pl.4, fig. 5). Cysts of *Protoperidinium nudum* are grouped with *Selenopemphix quanta* where they fall into its lower size range. Cysts of *P. nudum*? are only weakly polar compressed cysts of *Protoperidinium conicum* (see Wall and Dale, 1968).

Genus *Echinidinium* Zonneveld 1997 ex Head. Harland and Mattthiessen 2001

Echinidinium aculeatum

(Zonneveld, 1997)

(Plate 4, fig. 3)

Dimensions. Range of central body diameter: 16-30 μm; Range of processes length: 5-8 μm; Twenty-one specimens were measured (this study).

Distinguishing characters. Central body spherical, bearing randomly distributed processes. Central body wall is thin, pale brown, smooth with or without occasional isolated granules. Processes are hollow for most of length, distally tapering, circular in transverse section and with smooth surface. They are distally aculeate up to about four aculeae present on each process with aculeae up to 2 μm long and either unbranched or bifurcate. A few slender, solid processes occasionally also present. Archeopyle theropylic, apparently consisting of a split along a single suture (Original description in Zonneveld 1997). A simple split that may represent the archeopyle was observed on some specimens but the split could also be related to poor preservation rather than to an excystment aperture. No other tabulation reflected.

Echinidinium delicatum

(Zonneveld, 1997) ex Head. 2003

(Plate 4, fig. 1)

Dimensions. Range of central body diameter: 17-25 μm; Range of processes length: 2-4 μm.

Distinguishing characters. The cyst is light brown and has a smooth central body surface. Processes are hollow over one third to one half of their length, i.e. more conspicuously hollow than solid.

Echinidinium granulatum

(Zonneveld, 1997) ex. Head et al. 2001

(Plate 4, fig. 4)

Dimensions. Range of central body diameter: 20-46 μm; Range of processes length: 5-11 μm; Five specimens were measured (this study).

Distinguishing characters. The cyst wall is light brown and has granulated central body surface. Processes are hollow, acuminate, smooth and fine spinules can be present at the distal end. Processes bases are spherical to ovoidal (1/6-1/2 of processes length) and show a diameter of 1 to 5.5 μm.

Echinidinium transparantum

(Zonneveld, 1997)

(Plate 4, fig. 2)

Dimensions. Range of central body diameter: 22-36 μm; Range of processes length: 5-14 μm; Three specimens were measured (this study).

Distinguishing characters. The cyst wall is light brown and has a smooth central body surface. Processes are solid, acuminate and smooth. Processes bases are sub-spherical to irregularly rectangular with a diameter ranging from 1.5 to 2.5 μm.

Echinidinium sp.1

(Kielt, 2006)

(Plate 2, fig. 6)

Dimensions. Central body diameter: 22-28 μm; Process length: 5-9 μm; Seven specimens were measured (Kielt. 2006).

Distinguishing characters. The cyst is spherical and shows a smooth central body surface with occasional isolated granules. The central body wall is light brown and thin (1 μm). Processes are hollow, acuminate, smooth and solid at the distal end. They are regularly distributed. Their bases are spherical and large and show clear striations, quite similar to those of *Pheopolykrikos hartmanii* described by Matsuoka and Fukoyo (1986). However, *Echinidinium* sp.1 is much smaller and does not fall into the size range of *P. hartmanii*. No specimen with archeopyle indication has been observed yet. These specimens are thus informally assigned to the *Echinidinium* group.

Genus *Lejeunecysta* Artzner & Dörhöfer 1978 emend. Lentin & Williams 1976

Lejeunecysta sabrina

(Reid, 1977) Bujak 1984

Dimensions. Length: 58-90 μm (Reid, 1977)

Distinguishing characters. Dorsoventrally compressed cysts with peridinioid outline. The antapical horns are more-or-less symmetrical and tapering and are separated by an antapical depression that may be deep or shallow. The tips of the antapical horns may be smoothy rounded or have sharp points. The apical horn has a flattened tip and the apical pore area is thickened. The cyst wall is thin; single layered and has a microgranulate surface. There may be some faint lines of thinning along plate boundaries and the surface may be ornamented with longitudinal thickenings, striations or folds. Cingulum slightly indented and margins slightly thickened and raised. The archeopyle is intercalary (2a).

Biological affinity. *Protoperidinium leone*

Genus Quinquecuspis Harland 1977

Quinquecuspis concreta

(Reid, 1977; Harland, 1977)

(Plate 3, fig. 10)

Dimensions. Length: 60-80μm (Reid, 1977).

Distinguishing characters. Pentagonal cysts, dorsoventrally-compressed with well developed apical and antapical horns and a thick brown single-layered wall. The antapical horns are rounded and may be irregularly thickened at their tips. The surface is smooth or roughened and may show faint longitudinal lineations and low folds. The cingular margins are slightly raised and the sulcus is deeply indented and may show two depressions reflecting the flagellar pores. Archeopyle intercalary formed by loss of plate 2a, although an adjacent apical plate (3'?) is often also involved and there is frequent breakage of the cyst around the archeopyle.

Biological affinity. *Protoperidinium leone*

Genus *Selenopemphix* Benedek 1972 emend. Head 1993

Selenopemphix nephroides

(Benedek, 1972) emend. Bujak in Bujak et al. 1980

(Plate 3, fig. 6)

Dimensions. Diameter: 48-60 μm (Wall and Dale, 1968).

Distinguishing characters. Polar compressed cysts with an ovoidal to reniform outline in polar view. Wall light brown in color, single-layered and smooth. Apical and antapical horns

are low and have rounded terminations. Cingulum is strongly indented, so its margins appear flange-like in polar view. Archeopyle hexa-intercalary and formed by loss of plate 2a.

Biological affinity. *Protoperidinium subinerme*

Selenopemphix quanta

(Bradford, 1975) Matsuoka 1985

(Plate 3, fig. 7)

Dimensions. Central body width: 40-83 μm; Process length: 10-16 μm (Rochon et al., 1999).

Distinguishing characters. Cysts are polar compressed and are subcircular to slightly reniform in polar view. The wall is light to medium brown and smooth. Processes are solid except where they expand at their base and taper to sharp or blunt points. Processes occur along the cingular margins and also with variable density in rows on the epicyst and hypocyst, but do not occur in the sulcus. Archeopyle 2a intercalary elongated with rounded angles.

Biological affinity. *Protoperidinium conicum*

Genus *Stelladinium* Bradford 1975

Stelladinium spp.

(Plate 3, fig. 9)

Dimensions. Central body length: 30-47 μm; Process length: 8-21 μm; Five specimens were measured (this study).

Distinguishing characters. Cyst dorso-ventrally compressed having pentagonal outline with angles drawn into long horns of approximately equal length. Each horn is a solid process with a hollow base and tapers to a point. *Stelladinium* spp. has bifurcate processes. The cyst wall is single layered, brown pigmented and has a smooth surface. There may be a shallow sulcal groove. Archeopyle formed by an opening along the margins of plates 1a and 2a with the two opercular plates remaining attached to the cyst along their lateral margins. There is no other indication of tabulation. *Stelladinium* spp. differs from *Stelladinium redii* in having bifurcate processes.

Genus *Votadinium* Reid 1977

Votadinium calvum

(Reid, 1977)

(Plate 3, fig. 12)

Dimensions. Length: 54-72 μm (Reid, 1977).

Distinguishing characters. Cysts dorso-ventrally compressed with a strongly rounded peridinioid outline. The apical horn is represented by only a slight swelling and is greatly reduced so that the 2a intercalary archeopyle extends over the apex. Antapical horns are of approximately equal development and are separated by a shallow antapical depression. The wall is dark brown and a little less than 1 μm thick and is unthickened at the horns. The cyst surface is smooth.

Biological affinity. *Protoperidinium oblongum*

Votadinium spinosum

(Reid, 1977)

(Plate 3, fig. 11)

Dimensions. Length: 49 - 63 μm; Spine length: 3-7 μm (Reid, 1977).

Distinguishing characters. Heart shaped, compressed dorso-ventrally to half the width of the test with two antapical lobes separated by a shallow antapical depression in dorsal view and rounded apex. Wall thin with a smooth surface and ornamented by short solid spines which are usually curved. Archeopyle intercalary made by loss of plate 2A.

Biological affinity. *Protoperidinium claudicans*

Cyst A

(Plate 2, fig. 7)

Dimensions. Central body diameter: 20-33 μm; Process length: 4-9 μm (maximum width at the base varies from 1.0 μm to 4.0 μm); Fifteen specimens were measured (this study).

Distinguishing characters. In this study, specimens attributed to Cyst A occur in the Gulf of California and off the California coast and are occasionally observed along the western Mexican coast. They consist in small proximochorate cyst with a spherical to subspherical central body and numerous processes. The endophragm is thin and smooth and the cyst wall is light brown to golden-brown. Most processes are arranged in a linear or curved pattern that might be an indication of tabulation, but some processes are irregularly distributed over the entire surface of the cyst. Processes are mostly smooth although they can bear ridges at the base. Processes are hollow and have ribbon-like shape with a pointed termination. The outline of the process base is circular to irregularly rectangular in cross section. Most of processes are curved and are separated from each other at their base. However, occasionally, processes can be proximately fused. Their length is fairly constant for individual specimens.

The archeopyle seems to be theropylic and to involve loss of one or several precingular plates. Moreover, no specimen with clear archeopyle was observed yet. Cyst A has been also recorded in the surface sediments from the Georgia Strait (coastal region of British Columbia; Radi et al., 2007).

Biological affinity. Unknown

BIBLIOGRAPHIE

Alonso-Rodríguez, R., Ochoa, J. L., 2003. Nutrients, phytoplankton and harmful algal blooms in shrimp ponds: a review with special reference to the situation in the Gulf of California. Aquaculture 219, n°1-4, 317-336

Alonso-Rodríguez, R., Ochoa, J. L., 2004. Hydrology of winter-spring ''red tides'' in Bahía de Mazalán. Sinaloa, México. Harmful Algae 3, 163-171

Antoine, D., André, J.M., Morel, A., 1996. Oceanic primary production. 2. Estimation at global scale from satellite (coastal zone colour scanner) chlorophyll. Global Biogeochemical Cycle 10, 57-69

Antoine, D., Morel, A., 1996. Oceanic primary production. 1. Adaptation of a spectral light photosynthesis model in view of application to satellite chlorophyll observations. Global Biogeochemical Cycles 10, 43-55

Arellano-Torres, E., Machain-Castillo, M. L., Thunell, R., Keple, B., Mix, A., Lyle, M., Pisias, N., 2003. Glacial-Holocene changes in the upwelling regime of the Gulf of Tehuantepec, Mexico. Geophysical Research Abstracts 5, p. 13 958

Barron, J. A., Bukry, D., Bischoff, J. L., 2004. High resolution paleoceanography of the Guaymas Basin, Gulf of California, during the past 15 000 years. Marine Micropaleontology 50, 185-207

Behrenfeld, M., Falkowski, P., 1997. Photosynthetic rates derived from satellite based chlorophyll concentration. Limnology and Oceanography 42 (1), 1–20

Boumaggard, E. H., Gayet, J., Bobier, C., Machain-Castillo, M. L., Aguayo-Camargo, E., 1998. Distribution of sediments on the margin of the Gulf of Tehuantepec (East Pacific): Example of tectonic-eustatic interaction. Oceanologica Acta 21, n°1, 21-31

Coplen, T.B., 1995. Discontinuance of SMOW and PDB. Nature 375, 285

Dale, B., 1976. Cyst formation, sedimentation and preservation: factors affecting dinoflagellate assemblages in recent sediments form Tondheimsfjord, Norway. Review of Paleobotany and palynology 22, 39-60

Dale, B., 1977. New observations on *Peridinium faeroense* Paulsen (1905), and classification of small orthoperidinoid dinoflagellates. British Phycological Journal, 12: 241-253.

Dale, B., Fjellså, A., 1994. Dinoflagellate cysts as productivity indicators: state of the art, potential and limits. In: Zahn. R. (Ed.). Carbon Cycling in the Glacial Ocean: Constraints in the Ocean's Role in Global Change. Springer, Berlin, 521-537

Dale, B., 1996. Dinoflagellate cyst ecology: modeling and geological applications. In: Jansonius, J., McGregor, D.C, (Eds.). Palynology: Principles and Applications 3, Am. Assoc. Stratigr. Palynol. Foundation, College Station TX, 1249-1275

Dale, B., Dale, A. L., Jansen, F.J.H., 2002. Dinoflagellate cysts as environmental indicators in surface sediments from the Congo deep-sea fan and adjacent regions. Palaeogeography Palaeoclimatology Palaeoecology 185, 309-338

Dale, B., Thorsen, T. A., Fjellsa. A., 1999. Dinoflagellate Cysts as Indicators of Cultural Eutrophication in the Oslofjord, Norway. Estuarine, Coastal and Shelf Science 48, issue 3. 371-382

de Vernal, A., Bilodeau, G., Hillaire-Marcel, C., Kassou, N., 1992. Quantitative Assessment of Carbonate Dissolution in Marine Sediments from foraminifer Linings vs. Shell Ratios: Davis Strait, Northwest North Atlantic. Geology 20, 527-530

de Vernal, A., Eynaud, F., Henry, M., Hillaire-Marcel, C., Londeix, L., Mangin, S., Matthiessen, J., Marret, F., Radi, T., Rochon, A., Solignac, S., Turon, J.-L., 2005. Reconstruction of sea-surface conditions at middle to high latitudes of the Northern Hemisphere during the Last Glacial Maximum (LGM) based on dinoflagellate cyst assemblages. Quaternary Science Reviews 24, 897-924

de Vernal, A., Giroux, L., 1991. Distribution of organic-walled microfossils in recent sediments from the estuary and Gulf of St Lawrence. Canadian Special Publication of Fischeries and Aquatic Sciences 113, 189-199

de Vernal, A., Henry, M., Bilodeau, G., 1999. Techniques de préparation et d'analyse en micropaléontologie. Les Cahiers du GEOTOP, p.28

de Vernal, A., Henry, M., Matthiessen, J., Mudie, P.J., Rochon, A., Boessenkool, K., Eynaud, F., Grøsfjeld, K., Guiot, J., Hamel, D., Harland, R., Head, M.J., Kunz-Pirrung, M., Levac, E., Loucheur, V., Peyron, O., Pospelova, V., Radi, T., Turon, J.-L., Voronina, E., 2001. Dinocyst assemblages as tracer of sea-surface conditions in the northern North Atlantic, Arctic and sub-Arctic seas: the "n=677" database and derived transfer functions. Journal of Quaternary Science 16, 681-698

de Vernal, A., Larouche, A., Richard, P.J.H., 1987. Evaluation of palynomorph concentrations: do the aliquot and the marker-grain method yield comparable results? Pollen Spores 29, 291-303

de Vernal, A., Marret, F., 2007. Chapter Nine Organic-Walled Dinoflagellate Cysts: Tracers of Sea-Surface Conditions. Developments in Marine Geology 1, 371-408

de Vernal, A., Rochon, A., Turon, J.-L., Matthiessen, J., 1997. Organic-walled dinoflagellate cysts: palynological tracers of sea-surface conditions in middle to high latitude marine environments. Geobios 30, 905-920

Devillers, R., de Vernal, A., 2000. Distribution of dinoflagellate cysts in surface sediments of the northern North Atlantic in relation to nutrient content and productivity in surface waters. Marine Geology 166, 103-124

Douglas, R., Gorsline, D., Grippo, A., 2001. Late Holocene ocean-climate variations in Alfonso Basin, Gulf of California, Baja California, Mexico. Presented in agenda for Eighteenth Annual Pacific Climate Workshop, Abstract

Gaines, G., Elbraechter, M., 1987. Heterotrophic nutrition. In: Taylor, F.J.R. (Ed.). The biology of dinoflagellates. Blackwell Scientific, Oxford, 224–281.

Gibson, C.H., Thomas, W. H., 1995. Effects of turbulence intermittency on growth inhibition of a red tide dinoflagellate, *Folyaulax polyedra* Stein. Journal of Geophysical Research 100 (C12), 24841-24846

Gibson, C. H., 2000. Laboratory and ocean studies of phytoplankton response to fossil turbulence. Dynamics of Atmospheres and Oceans 31, 295-306

Hamel, H., de Vernal, A., Gosselin, M., Hillaire-Marcel, C., 2002. Organic-walled microfossils and geochemical tracers: sedimentary indicators of productivity changes in the North Water and northern Baffin Bay during the last centuries. Deep-Sea Research II 49, 5277-5295

Head, M.J., 1996. Modern dinoflagellate cysts and their biological affinities. In: Jansonius, J., Mc Gregor, D. C. (Eds.). Palynology: Principles and Applications, vol. 3, AASP Foundation, Salt Lake City, UT, 1197-1248

Jacobson, D., Anderson, D., 1986. Thecate heterotrophic dinoflagellates: feeding behaviour and mechanics. Journal of Phycology 22, 249-258

Kessler, W. S., 2006. The circulation of the eastern tropical Pacific: A review. Progress in Oceanography 69, 181-217

Kielt, J-F., 2006. Distribution des assemblages palynologiques et microfaunistiques le long des côtes Ouest mexicaines. Université du Québec à Montréal

Lewis, J., Dodge, J. D., 1987. The cyst-theca relationship of *Protoperidinium americanum* (Gran & Braarud) Balech. *Journal of Micropalaeontology*, 6: 113-121

Lewis, J., Dodge, J. D., Powell, A. J., 1990. Quaternary dinoflagellate cysts from the upwelling system offshore Peru, Hole 686B, ODP Leg 112. In: Suess, E., von Huene,

R., et al. (Eds). Proceeding of the Ocean Drilling Program, Scientific Results, vol. 112, 323-327

Lewis, J., Hallett, R., 1997. *Lingulodinium polyedrum* (*Gonyaulax polyedra*) a blooming dinoflagellate. Oceanography and Marine Biology Annual Review 35, 97-161

Marret, F., 1994. Distribution of dinoflagellate cysts in recent marine sediments from the east Equatorial Atlantic (Gulf of Guinea). Review of Paleobotany and Palynology 84, 1-22

Marret, F., Zonneveld, K, 2003. Atlas of modern organic-walled dinoflagellate cyst distribution. Review of Palaeobotony and Palynology, vol. 125, n°1-2, 1-200

Matsuoka, K., 1985. Archeopyle structure in modern Gymnodinialean dinoflagellate cysts. Review of Palaobotany and Palynology, 44: 217-231

Matsuoka, K., Fukuyo, Y., 1986. Cyst and motile morphology of a colonial dinoflagellate *Phaeopolykrikos harmannii* (Zimmermann) comb. nov. Journal of Plankton Research, 8: 811-818

Matsuoka, K., Kawami, H., Nagai, S., Iwataki, M., Takayama, H., 2009. Re-examination of cyst–motile relationships of *Polykrikos kofoidii* Chatton and *Polykrikos schwartzii* Bütschli (Gymnodiniales, Dinophyceae). Review of Palaeobotany and Palynology, volume 154, Issues 1-4 : 79-90

Matthews, J., 1969. The assessment of a method for the determination of absolute pollen frequency. New Phytologist 68, 161-166

Mee, L.D., Cortés-Altamirano, Ramírez-Flores, A., Flores-Verdugo, F., González Farías, F., 1985. Coastal upwelling and fertilty of the southern Gulf of California: Impact of the 1982-1983 ENSO event. Tropical Ocean-Atmosphere Newsletters 31, 9-10

Meyers, P.A., 1994. Preservation of elemental and isotopic source indentification of sedimentary organic matter. Chemical Geology 144, 289-302

Meyers, P.A., 1997. Organic geochemical proxies of paleoceanographic, paleolimnologic and paleoclimatic processes. Organic Geochemistry, Vol. 27, 213-250

Monreal-Gómez, M. A., Salas-de-León, D. A., 1998. Dinámica y estructura termohalina. El Golfo de tehuantepec: el ecosistema y sus recursos,Vol. 2, 13-26

O'Leary, M. H., 1988. Carbon isotopes in photosynthesis. Bioscience 38, 328-336

Ortiz-Lozano, L., Granados-Barba, Solís-Weiss, García-Salgado, 2005. Environmental evaluation and development problems of the Mexican Coastal Zone. Ocean & Coastal Management 48, 161-176

Pospelova, V., de Vernal, A., Pedersen, T. F., 2008. Distribution of dinoflagellate cysts in surface sediments from the northeastern Pacific Ocean (43–25°N) in relation to sea-surface temperature, salinity, productivity and coastal upwelling. Marine Micropaleontology 68, 21–48

Radi, T., de Vernal, A., 2004. Dinocyst distribution in surface sediments from the northeastern Pacific margin (40-60°N) in relation to hydrographic conditions, productivity and upwelling. Review of Palaeobotany and Palynology 128, 169-193

Radi, T., de Vernal, A., 2008. Dinocysts as proxy of primary productivity in mid-high latitudes of the Northern Hemisphere. Marine Micropaleontology 68, 84-114

Radi, T., Pospelova, V., de Vernal, A., Barrie, J. V., 2007. Dinoflagellate cysts as indicators of water quality and productivity in British Columbia estuarine environments. Marine Micropaleontology 62, 269–297

Reid, P. C., 1974. Gonyaulacean dinoflagellate cysts from the British Isles. Nova Hedwigia, 25: 579-637

Reid, P. C., 1977. Peridiniacean and glenodiniacean dinoflagellate cysts from the British Isles. Nova Hedwigia, 29: 429-463.

Rochon, A., de Vernal, A., Turon, J. L., Matthiessen, J., et Head, M.J., 1999. Distribution of dinoflagellate cysts in surface sediments from the North Atlantic Ocean and adjacent basin and quantitative reconstruction of sea-surface parameters. American Association of Stratigraphic Palynologists, Dallas, Contribution Series, n°35, pp. 152

Ruiz-Fernàndez, A.C., Páez-Osuna, F., Machain-Castillo, M.L., Arellano-Torres, E, 2004. ^{210}Pb geochronology and trace metal fluxes (Cd, Cu and Pb) in the Gulf of Tehuantepec, South Pacific of Mexico. Journal of Environmental Radioactivity 76, 161-175.

Targarona, J., Warnaar, J., Boessenkool, K.P., Brinkhuis, H., Canals, M., 1999. Recent dinoflagellate cyst distribution in the North Canary Basin, NW Africa. Grana 38, 170-178

Taylor, F.J.R., Pollingher, U.,1987. The ecology of dinoflagellates. In: Taylor, F.J.R. (Ed.). The biology of Dinoflagellates. Blackwell Scientific Publications, Oxford. pp. 398–529

Thibodeau, B., de Vernal, A., Mucci, A., 2006. Recent eutrophication and consequent hypoxia in the bottom waters of the Lower St. Lawrence Estuary: Micropaleontological and geochemical evidence. Marine Geology 231, 37-50

Vásquez-Bedoya, L.F., Radi, T., Ruiz-Fernandez, A.C., de Vernal, A., Machain-Castillo, M.L., Kielt, J.F., Hillaire-Marcel, C., 2008. Organic-walled dinoflagellate cysts and

benthic foraminifera in coastal sediments of the last century from the Gulf of Tehuantepec, South Pacific Coast of Mexico. Marine Micropaleontology 68, pp. 49-65

Wall, D., 1965. Modern hystrichospheres and dinoflagellate cysts from the Woods Hole region. Grana Palynologica, 6: 297-314

Wall, D., Dale, B., 1968. Modern dinoflagellate cysts and evolution of the Peridiniales. Micropaleontology, 14: 265-304.

World Ocean Atlas, 2001. CD-ROMs data set, National Oceanographic Data Center, Silver Spring, MD

Zonneveld, K.A.F., 1997. Dinoflagellate cyst distribution in surface sediments from the Arabian Sea (northwestern Indian Ocean) in relation to temperature and salinity gradients in the upper water column. Deep-Sea Research II 6-7, 1411-1443

Zonneveld, K. A. F., Versteegh, G. J. M., de Lange, G. J., 2001. Paleoproductivity and post-depositional aerobic organic matter decay reflected by dinoflagellate cyst assemblages of the Eastern Mediterranean S1 sapropel. Marine Geology, 172(3-4), 181-195